Macromolecules

pubs.acs.org/Macromolecules
Article

Preparation of Organogel Beads for Smart Valve Components: Kinetic Study of Their Chemoresponsiveness

Johannes Gmeiner, Jonah Hasse, Gerrit A. Luinstra,* Kathrin M. Eckert, and Irina Smirnova

Cite This: *Macromolecules* 2026, 59, 8403−8419
Read Online

ACCESS | Metrics & More | Article Recommendations | Supporting Information

ABSTRACT: Chemoresponsive P(NiPAAm-*co*-AA) beads (approximately 3 mm radius) were synthesized via UV-light-induced copolymerization of *N*-isopropylacrylamide (NiPAAm) and acrylic acid (AA) in aqueous droplets suspended in silicone oil. SEM analysis revealed a closed surface for beads with a 3-fold excess of AA; macroporous morphologies appeared for NiPAAm:AA ratios of 1:1 and 3:1. Swelling behavior was mapped across linear alcohols, acids, esters, and their mixtures, revealing a cononsolvency related to ethanol presence. Beads with a 1:1 monomer ratio exhibited the largest swelling difference between ethanol and ethyl acetate or with mixtures of ethyl acetate and ethanol. Their reversible swelling−shrinkage was fitted to two exponential functions. The time constant of the first fast part is on the order of minutes. The extent of shrinkage is negatively correlated with the logarithmic ethanol fraction in ethyl acetate. Beads in a casing were used to halt the flow of ethyl acetate after a switch to ethanol.

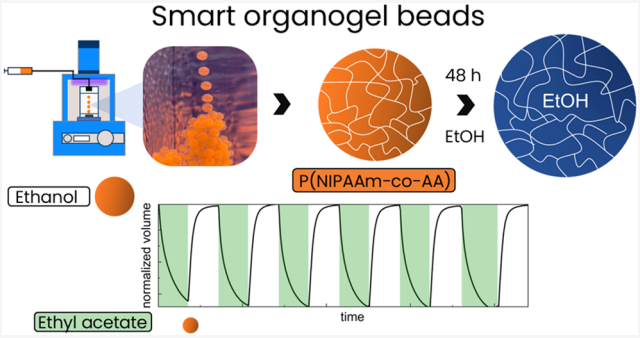

INTRODUCTION

The development of smart gels, i.e., gels with an ability to reversibly change their shape in response to some kind of external stimulus, is an appealing field of research that is actively pursued.[1−10] Smart gels are relevant for various biomedical applications,[11] including targeted drug release,[12−15] tissue engineering, and cell immobilization.[16−21] Hydrogels, especially those synthesized from *N*-isopropylacrylamide (NiPAAm)[22−26] and acrylic acid (AA),[27−33] have been in spotlight for quite some time (past 20 years) because of their 2-fold, i.e., thermo- and pH-responsive, properties. These properties make them also relevant for applications in chemical engineering, such as in the development of smart valve systems.[34−37] A smart valve will be understood as a general device that contains a responsive gel, which undergoes a change of volume upon a chemical trigger (change of medium).[38−40]

Fluid flow control is central to controlling many liquid-based chemical processes, where precise tuning of conditions can increase selectivity and optimize space−time yields.[4,41] A conventional setup with addressable valves will only be effective when the operation is in an environment with detectors, allowing for a process-control-system-regulated operation. Such valves themselves do not adapt to changes in the system. The latter can be a limitation, certainly with a dynamically changing composition during the progress of a reaction. Autonomous valves with a "smart" organogel as a directing component would allow an action that regulates flow rates without the need for detectors and external control systems.[42] The "smartness" of the gel could involve the ability to swell or shrink in response to a (reacting) medium. The development of such "inherent" smart entities may lead to innovations in a variety of scientific and industrial fields, including (bio)chemical process control, lab-on-a-chip technologies,[43,44] agriculture,[36] and environmental monitoring[11] systems.[9] The inherent soft mechanical responses are also very much of relevance in a biological context.[18,45]

The description of the response of a gel to different stimuli is still in need of a deeper understanding: its action should be predictable at a useful level for an application.[46−48] A spherical shape provides a consistent response to stimuli from all directions, unlike other shapes such as cylinders or plates.[49] Round organogel beads thus seem well-suited as smart valve model components, particularly in experimental studies: their spherical shape gives a uniform and isotropic swelling that is also relatively easy to describe.[50,51] And in practice, a round bead in a round channel is expected to show an isotropic expansion or contraction on the action of the stimulus, thereby potentially regulating the flow efficiently.[4] The regular surface structure of such beads promotes a uniform interaction with

Received: April 6, 2026
Revised: July 9, 2026
Accepted: July 10, 2026
Published: July 20, 2026

Scheme 1. Organogel Preparation in Droplets Comprising Dropwise Addition of Aqueous Monomer Solution to Silicon Oil, UV-Light-Induced Radical Polymerization, and Solvent Exchange

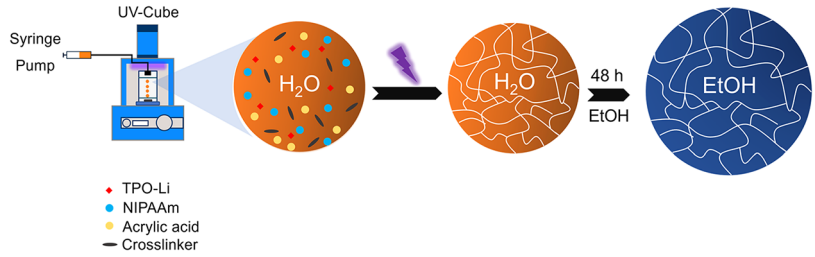

the surrounding medium, shortening swelling, and shrinkage times.[40] The shape of a sphere also seems beneficial to withstand mechanical stresses, e.g., those under high flow.[52]

The state of the art of "smart" hydrogels comprises a response to a change of temperature,[40,53,54] pH value,[34,35,55−57] to light,[58−60] or to CO_2.[61−63] Triggering a response by a change of a general chemical composition (other than pH values or CO_2 and beyond water as medium[40]), certainly in the context of a smart valve, seems not to have had a large focus.[40,64] Smart gels with chemoresponsive properties would, however, be more of universal value in a valve application.[40,47,65,66]

This study concerns the synthesis of P(NiPAAm-*co*-AA) organogels in the form of round beads and the analysis of their response to changes in organic solvents and solvent mixtures. Round beads in the millimeter range were obtained by droplet polymerization. An acrylic precursor aqueous solution was dripped into a silicone oil, where UV-light triggered polymerization while the forming beads sank slowly to the bottom. The process not only provides control over the size but also ensures high reproducibility in the preparation of spherical particles (Scheme 1; a related thermal polymerization to beads was reported before[67]). The production process of the hydrogel beads used in this work thus differs from conventional methods such as sedimentation polymerization[67] (falling drop),[68] alginate techniques,[69−72] and others.[73] The simple approach opens up possibilities for the production of polymer particles of multifaceted functionality in the millimeter range, expanding the options beyond microgels.[74] In the case of hydrogels, a large degree of synthetic freedom allows the properties to be tailored for application in complex systems that need a specific sensitivity.

It will be shown that thermoresponsive and pH-sensitive hydrogels for (autonomous microfluidic) flow control can be pushed to include solvent-quality-based responsiveness in organic media. The synthesized organogels exhibit a useful degree of swelling in alcohol and shrinkage in aliphatic esters. Such a property gives the option to use them as an autonomous valve component in a setup for the preparation of esters from alcohols and acids. The intermediate swelling in mixtures of solvents such as in the course of an esterification is of relevance too. It is mentioned that in the case of solvent mixtures, a cosolvency and, more prominent in this study, a noncosolvency may arise. The latter describes a situation wherein a polymer is (more) soluble in the single components making up the mixture than in the mixture. The microscopic origin of cononsolvency is still a matter of debate.[75,76] It has been pointed out that interactions between the components of the mixture are competing with interactions between the polymer segments. This may lead to more solvent−solvent and in consequence more polymer−polymer interactions.[77] A further line of arguments is that cononsolvency could arise from the preferential binding of one of the components of the solvent mixture (also on account of temporary cross-link formation by hydrophobic aggregation in PNiPAAm but which is also questioned as a cononsolvency may principally arise in ternary mixtures).[78−87] It indeed is found as a preliminary result here that one organogel shows a cononsolvency in solvent mixtures with ethanol.

EXPERIMENTAL SECTION/METHODS

Materials and Equipment

Acetic acid (Sigma-Aldrich, 82024 Taufkirchen, Germany), acrylic acid (Synthopol Chemie, 21614 Buxtehude, Germany), ARACO-200 LEMON UV Pigment (ARALON COLOR GmbH, 56412 Heiligenroth, Germany), butan-1-ol (Sigma-Aldrich, 82024 Taufkirchen, Germany), butyric acid (Grüssing GmbH, 26849 Filsum, Germany), dimethyl sulfoxide-d_6 99.5 atom % (Sigma-Aldrich, 82024 Taufkirchen, Germany), ethanol absolute ≥ 99.8% (VWR Chemicals, 64295 Darmstadt, Germany), ethyl acetate (BCD Chemie GmbH, 21079 Hamburg), lithium-phenyl-2,4,6-trimethylbenzoylphosphinat ≥ 95% (Sigma-Aldrich, 82024 Taufkirchen, Germany), methanol (VWR Chemicals, 64295 Darmstadt, Germany), *N*,*N*′-methylene bis(acrylamide) ≥ 98% (Sigma-Aldrich, 82024 Taufkirchen, Germany), *N*-isopropylacrylamide 97% (Thermo Scientific Chemicals), pentanoic acid (TCI Deutschland GmbH, 65760 Eschborn, Germany), propan-1-ol (VWR Chemicals, 64295 Darmstadt, Germany), propanoic acid (TCI Deutschland GmbH, 65760 Eschborn, Germany), and silicone oil M 200 (Carl Roth, 76185 Karlsruhe, Germany) were used.

Characterization

Fourier-Transform Infrared (FTIR) Spectroscopy. ATR-FTIR spectra of the samples were recorded using a Shimadzu IR Spirit with QATR-S Unit (Shimadzu Deutschland GmbH, Duisburg, Germany). The measurements were conducted over a spectral range of 4000−400 cm^{-1} with a resolution of 2 cm^{-1}, utilizing 15 scans.

Morphological Characterization. Morphological evaluation of the gel networks was achieved after the gels were frozen in liquid nitrogen after synthesis and then lyophilized at −90 °C and 0.250 mbar for 48 h (γ 2-16LSCplus, Osterode am Harz, Germany). The dried gels were crushed and sputter-coated with a thin Pt layer. The analysis is by scanning electron microscopy at 5 kV high voltage (LEO Electron Microscopy Inc., One Zeiss Drive, Thornwood, NY 10594, USA). The size distribution of the beads was determined using three independent samples. The photos for this were taken in a photo box (Godox LST40), and the beads were placed in the respective solvent; 100 beads each were evaluated by using ImageJ (manual selection). Pore size analysis was performed using ImageJ image analysis software.

Nuclear Magnetic Resonance (NMR) Spectroscopy. The relative solvent composition within the gel network after syneresis was determined by crushing blotted organogel beads that were flash-frozen in liquid nitrogen. The resulting gel fragments were transferred into vials containing DMSO-d_6 and agitated on a shaker for 1 h to affect dissolution of the gelator matrix and quantitative extraction of

https://doi.org/10.1021/acs.macromol.6c00960
Macromolecules 2026, 59, 8403−8419

the trapped solvents. ^{1}H -NMR spectra of the DMSO-d_6 solutions were obtained using a Bruker (Billerica, MA, USA) Avance I−III 400 MHz or a Bruker Avance I 500 MHz spectrometer at a temperature of 298 K. The chemical shift (δ) was expressed in parts per million (ppm) relative to the internal standard, tetramethylsilane (TMS) at δ = 0.00 ppm. The relative weight percentages (wt %) of ethanol and ethyl acetate were calculated by integration of the signals of the respective aliphatic CH_3 resonance (triplet at δ = 1.06 ppm for ethanol, respectively, singlet at δ = 1.99 ppm for ethyl acetate).

Preparation of the Hydrogel-Precursor Solution

The precursor solution was prepared by adding a total amount of 4 g of monomers (20 wt % in total of acrylic acid and NiPAAm in different ratios; Table 1) to 16 mL of water (80 wt %) and stirring.

Table 1. Monomer Composition of the Hydrogel-Precursor Solution

entry	organogel	NiPAAm [wt %]	AA [wt %]
1	OG15-5	15	5
2	OG10-10[a]	10	10
3	OG5-15	5	15

[a]FTIR analysis of NIPAAM, AA, and the resulting P(NIPAAm-*co*-AA) is in accordance with complete conversion (Figure S1).

Cross-linker *N*,*N*-methylene bis(acrylamide) (MBA; 60 mg; 0.3 wt %) and photoinitiator TPO-Li (20 mg; 0.1 wt %) were added and dissolved by vigorous stirring. The precursor solution was degassed under atmospheric pressure using ultrasound for 5 min. The swelling behavior of transparent gels was evaluated by in-line volume tracking on gels with additional fluorescent pigment ARACO-200 LEMON (5 mg, 0.025 wt %).

UV-Droplet Polymerization Method for the Fabrication of Hydrogel Beads

Hydrogel beads were prepared in 250 mL of silicone oil (ρ of 0.975 g·cm^{-3}) confined to a beaker placed in a reflective chamber (180 × 180 × 180 mm^3) with a UV-light source (irradiation intensity up to 1.100 mW/cm^2 at a wavelength of 365 nm). The OEM chamber was modified to allow tubing to pass through the hatch door. The precursor solution was dropped into the silicone oil at a constant flow rate of 3 mL/min through PTFE tubing (1.6 mm inner diameter) using a syringe pump (LongerPump Model LSP02-1B equipped with a 20 mL HENKE-JECT Syringe). The droplets sink slowly and polymerization is basically completed within 30 s. The hydrogel beads were collected on a Büchner funnel and washed with ethanol (3 × 100 mL).

Swelling Experiments of Organogel Beads

Gravimetric Determination of the Degree of Swelling (DoS). The gels were equilibrated in the reactants and products of an esterification, i.e., in alcohols, acids, and esters. Freshly prepared hydrogels from aqueous solutions were immersed in 250 mL of ethanol for 24 h at room temperature (while stirring slowly). They were transferred to a further portion of ethanol and held there for another 24 h.

The equilibrium swelling values in alcohols, carboxylic acids, their mixtures, and esters were obtained after 48 h in a medium. The organogels were then freeze-dried at −90 °C under high vacuum (0.250 mbar) for 72 h. The mass-specific degree of swelling DoS was calculated as DoS = $\text{mass}_{\text{swollen gel}}/\text{mass}_{\text{dried polymer}}$. The rate of swelling was obtained by transferring the gel beads from 100 mL volumes of, e.g., ethanol to ethyl acetate or to its mixtures with ethanol or acetic acid. This exchange was generally carried out over several cycles of 30 min each.

Volumetric Tracking of the Swelling Behavior by Inline Monitoring. The volumetric swelling behavior of the hydrogel beads was recorded at 25 °C using interactive image processing. The beads were fixed inside a 100 mL cuvette sealed with a 3D-printed lid. Their size was recorded using a camera over several cycles of 60 min consisting of 30 min of shrinkage in not as good solvent (mixture) and 30 min of swelling in the better one. Images were taken every 30 s to ensure a high resolution of the tracking. The resulting image series was evaluated with a Python script developed for counting the pixels corresponding to the bead circumference in a fixed space. The script identified color differences between the bead and the background, isolated the region of interest (ROI), and determined the bead diameter using contour detection. The pixel-based diameters were used to calculate the radius and volume of the beads.

Valve Actuation Experiment

A custom-made glass flange casing (70 mm height, 25 mm inner diameter) was filled with 25 g of ethyl acetate-wet OG10-10 organogel beads. An integrated stainless steel mesh (1 mm pore size) retained the beads inside the transparent boundary. The valve was connected to the bottom of a reservoir containing solvent. The solvent was allowed to leave the reservoir in a free flow from the bottom through the valve. A diaphragm metering pump (ProMinent delta optoDrive, Heidelberg, Germany) with a maximum delivery rate of 160 strokes per minute and a maximum flow rate of 30 L·h^{-1} was used to keep the level in the reservoir at a constant height, taking the solvent from a collection vessel below the valve. The loop contained a total 350 mL of solvent.

RESULTS AND DISCUSSION

Preparation and Characterization of Organogel Beads

Gel beads composed of acrylic acid and NiPAAm were obtained in an aqueous medium using radical droplet polymerization at room temperature. Three formulations were used with 5−15 wt % of the respective monomers, always adding up to 20 wt % of monomer content. *N*,*N*′-methylene bis(acrylamide) (MBA; 0.3 wt %) was added as a cross-linker, and lithium-phenyl-2,4,6-trimethyl benzoylphosphinate (TPO-Li) was the choice of photoinitiator. The organogel products OG*x*-*y* carry numbers *x* and *y*, the first one corresponding to the wt % of NiPAAm, the second to wt % of AA (Table 1). The copolymerization parameters of the NiPAAm/AA system in water have estimated values of r_1 of 14 and r_2 of 0.07.[88] These numbers imply that blocky structures are formed in the batch polymerization inside the droplet as minireactor, NiPAAm being consumed much faster.[88] Core−shell type of NiPAAm-AA microgels, mostly with less than 10 wt % AA, are formed in emulsion or seed polymerization:[89−91] These products tend to have PNiPAAm-like properties, compatible with the presence of larger PNiPAAm domains: e.g., a LCST (lower critical solution temperature) is detected in a small temperature range.[92−94] It has been noted too that the product of the copolymerization parameter is close to one, implying a constant rate of incorporation of both monomers.[95] Arguments for the formation of fractal (blocky) structures of NiPAAm-AA copolymers have accordingly been put forward in the case of copolymers with a lower ratio of monomers.[96]

The small ratios of NiPAAm to AA (3 to 1/3) used here in the gel preparation are not common; however, most studies concern PNiPAAm-AA copolymers (also as microgels) with a ratio larger than 10.[33,91,92,94,97−104] The low ratios in this initial study were chosen with the objective to map the response to a change of medium over a larger range of compositions. Studies on PNiPAAm-AA copolymers with a lower ratio of NiPAAm to AA show additional features, which arise from substantial interactions between different polymer segments.[32,93,96,105−108] The latter is also documented for blends of PNiPAAm and PAA.[109] It was also inferred that the PAA entities might separate from the hydrophobic PNiPAAm domains when they

https://doi.org/10.1021/acs.macromol.6c00960
Macromolecules 2026, 59, 8403−8419

Scheme 2. Radical Copolymerization of NiPAAm and Acrylic Acid Induced by Irradiation of TPO-Li and with MBA as the Cross-Linker: Images of (a) OG10-10 and (b) OG5-15 on a Metal Skewer

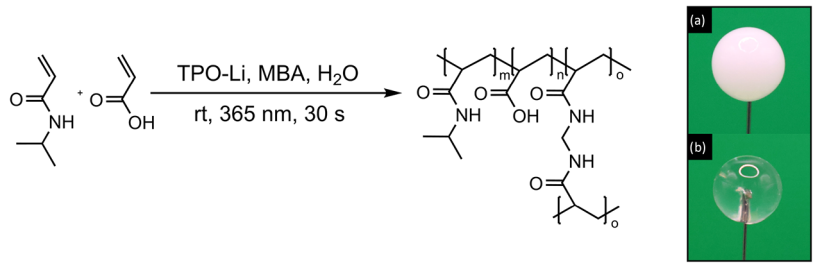

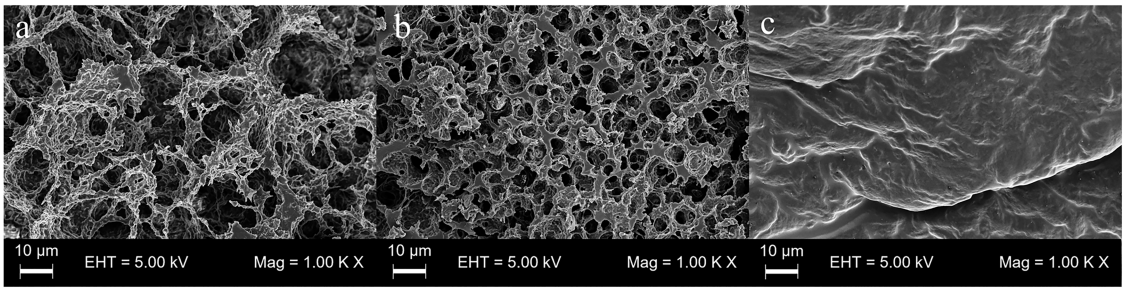

Figure 1. SEM images of hydrogel beads with NiPAAm:AA wt% ratios of (a) 15:5, (b) 10:10, and (c) 5:15 after freeze-drying from water.

can form in the specific arrangement of the monomers.[93,96,101,107,110,111]

Droplets of the precursor solution were generated by pumping it slowly through tubing that ends just above the surface of a medium-viscous silicone oil (unstirred) in a glass beaker. The beaker is located in a chamber ($18 \times 18 \times 18$ cm^3) with reflective walls and can be illuminated by an LED UV source. The initiation of the polyreaction, induced by the UV source at an intensity of 880 mW·cm^{-2} and a wavelength of 465 nm, transformed the droplets into uniform beads within 30 s. This is within the time of sedimentation of the droplet to the bottom (Scheme 1). The beads with 15 and 10 wt % of NiPAAm in the precursor solution immediately turn opaque as the copolymerization sets in. This is in contrast to the expectation of a clear PNiPAAm containing hydrogel formed below its LCST.[112] This observation is more compatible with the formation of a cross-linked system as reported for fast NiPAAm/AA copolymerization.[88,113] Indeed, it is found that the UV-induced droplet copolymerization, of e.g., equimolar amounts of NiPAAm and AA, also leads to round beads with some mechanical stability in the absence of the cross-linker, as was reported before for copolymerization in aqueous solution (contrasting, e.g., redox-initiated copolymerization of NiPAAm and AA).[114] Latter opaque beads appear softer and less tough, disintegrating under little pressure.

Heating to 70 °C or cooling to 0 °C of the OG15-5 or the OG10-10 beads (Table 1, entry 1, 2) does not lead to a transparent gel. The OG5-15 gel in contrast remains clear throughout its formation and also is transparent at the end. The OG5-15 gel is faintly opaque at 50 °C in water, possibly showing that NiPAAm domains precipitate. The PNiPAAm segments in the OG5-15 apparently can form a separate phase (vide infra) in the range of the wavelength of visible light. The PNiPAAm-related phase transition (LCST at about 32 °C) correspondingly shifted to a higher temperature with the AA content.[115] A visual detection is not always successful and compatible with the faint opaqueness that arises.[32,105] Such subtle changes in appearance can of course not be detected in the turbid OG15-5 and OG10-10, but structural changes may occur (vide infra).[96,116]

The water in the beads was subsequently exchanged for ethanol, in line with the objective to study them in organic media. Some solvents of this study have a low solubility in water and vice versa, which would complicate the direct exchange in the originally formed hydrogels. OG15-5 and OG10-10 gels with the higher NiPAAm content remain opaque in ethanol (Scheme 2, image a). This is in contrast to PNiPAAm gels, which tend to be soluble in neat low-mass alcohols.[117] The observations during the copolymerization already hinted toward the formation of more densely cross-linked domains inside the beads. Chain segments inside these domains apparently cannot be solvated to a substantial degree, i.e., to reach a matching index of reflection, neither in water nor in alcohol. In contrast, the more hydrophilic AA-rich aqueous gel OG5-15 yields a transparent system in ethanol too (Table 1, entry 3; Scheme 2, image b). The inner structure of this type of bead is markedly different: the transparency in two solvents is compatible with a complete solvation of chain segments.

The particle size of the beads of about 5 mm diameter can be satisfactorily described as normally distributed. The sigma values of the distribution are well below 10% of the mean (Figure S2). The beads are smaller in water than in ethanol, and on average, the size increased by 40−50% after exchange to ethanol. The increase in size is congruent to the AA content, which can be explained by either a lower cross-link density for gels with more AA or to AA-based copolymer chain segments with a better solubility in ethanol.

The behavior of NiPAAm copolymers and gels can be quite complex, with no exception here.[31,51,118−121] The solubility of PNiPAAm in alcohols results from specific (hydrogen-bond-based) interactions of the amide to the solvent.[76,78,80,83,122−124] The solubility of the copolymers is less easy to describe. The copolymers of NiPAAm and AA may contain several types of polymer−polymer segment interactions, which enthalpically compete with interactions to the medium. Also, the cross-

https://doi.org/10.1021/acs.macromol.6c00960
Macromolecules 2026, 59, 8403−8419

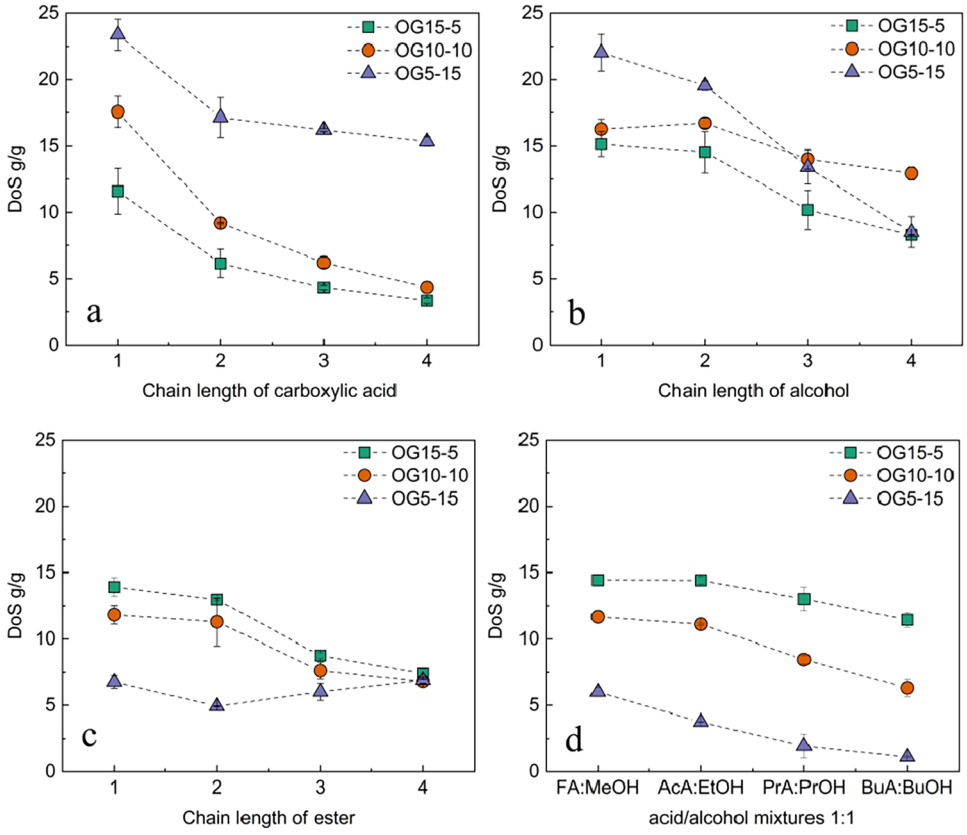

Figure 2. Gravimetric degree of swelling (DoS) of the gels in (a) carboxylic acids, (b) alcohols, (c) esters, and (d) acid/alcohol 1:1 mixtures (ester: 1: methyl formate, 2: ethyl acetate, 3: propyl acetate, 4: butyl acetate, FA: formic acid, AcA: acetic acid, PrA: propionic acid, BuA: butyric acid).

linked structure may hinder the formation of hydrophobic interactions between polymer segments.[94] Beads of OG10-10 in water do not show a typical jump in size when cooled from 50 °C to room temperature (Figure S3). Rather, their size monotonously increases at least to 25 °C: the copolymer segments increase their interactions with water. This behavior is compatible with the presence of NiPAAm-rich domains with LCST behavior of various sizes and/or compositions and with the presence of cross-links that hinder coherent segment movements.[99] The relatively high AA content of such copolymers may have led to substantial interactions between the acid (protonated form would prevail in ethanol) and the amide entities, changing the internal structure away from a majority of amide−amide hydrophobic interactions of a PNiPAAm, as was suggested before.[97] The cross-link density may also be a cause for differences in the organogels; however, since the mechanical properties were not studied yet, no information on this is available.

Morphological Characterization of OG Gels

SEM images of the freeze-dried samples (from water) of various beads reveal open-pore structures for the NiPAAm-rich, turbid gels OG15-5 and OG10-10, whereas the OG5-15 bead has a closed surface (Figure 1). Although the freeze-drying procedure of the sample preparation will change the pore size, structural differences in these closely related materials are probably conserved. The macroreticular structure of the OG15-5 gel is coarser than that of the OG10-10 gel. The dried OG15-5 shows large interconnected pores of an average pore size diameter (PSD) of 11.5 ± 1.6 μm (Figure 1a) in high vacuum and OG10-10 has a finer porous structure with an average PSD of 4.4 ± 1.4 μm after freeze-drying. Such open-pore structures are favorable for solvent exchange and swelling, and beads of that kind seem a good choice for the purpose of this study (microscopic images of OG10-10 in ethanol or ethyl acetate indicate windows of sizes of 3−7 μm in ethyl acetate resp ethanol; Figure S4).

Similarly structured NiPAAm gels were generated by performing radical polymerization in a mixture of water and methanol, which proceeds by intermediate polymer precipitation (phase separation) on the basis of the cononsolvency effect[49,74,125] or by polymerizations in a medium with a higher ionic strength,[126] and by γ-ray-induced NiPAAm-AA copolymerization above the LCST.[108,127] Dense structures are initially generated that become loosely connected in the progress of batch copolymerization. This outcome is also predicted (and observed)[128] by, e.g., the diffusion-limited aggregation of sol particles in dependence of the rate of gel formation.[114] It was shown that a fast initiation of the copolymerization—like that by UV radiation—will lead to more dense domains that are loosely connected (with an overall lower cross-link density).[94,129] The extensive generation of radicals by the photoinitiation will result in a high radical concentration with fast propagation and termination. Transfer-to-chain reactions will lead to local cross-links in dependence of the respective rates, i.e., next to those generated from the cross-linker.[88] The gel particles will tend to phase-separate in an early stage of monomer conversion. The importance of the polymerization rate for phase separation of intermediate gel particles of PNiPAAm is documented.[130] A similar effect is described for such copolymers prepared from a formulation with a higher cross-linker content of 3−5 wt %.[131] In

https://doi.org/10.1021/acs.macromol.6c00960
Macromolecules 2026, 59, 8403−8419

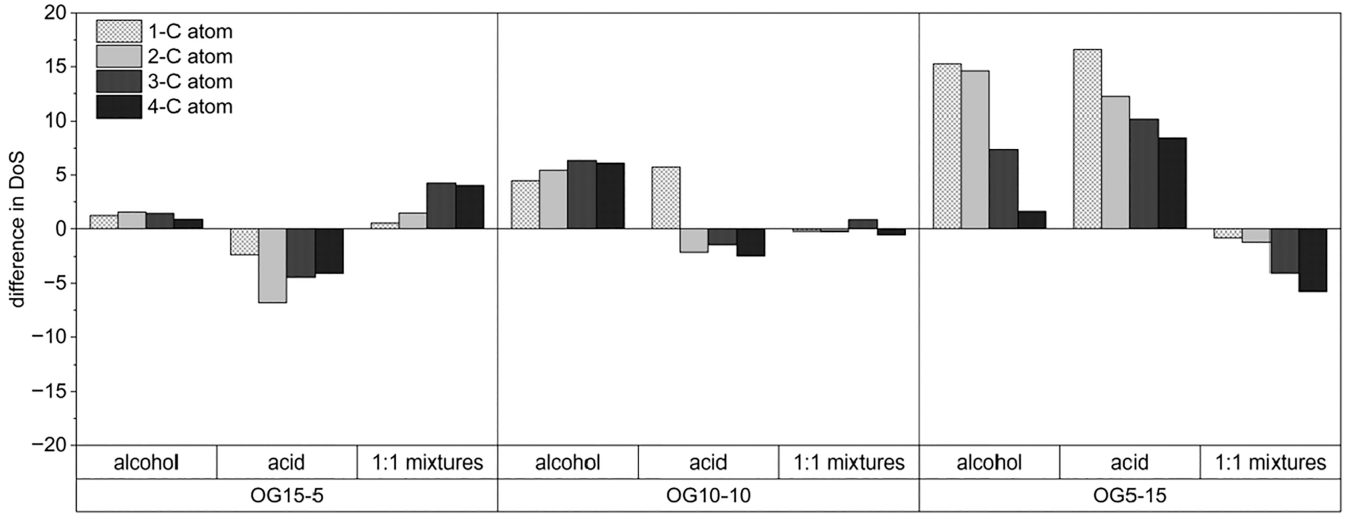

Figure 3. Difference of DoS in alcohols, acids, and their 1:1 mixtures to the corresponding esters.

accordance, the gel from equal amounts of NiPAAm and AA (OG10-10) has a finer structure, indicative of a slower polymerization and/or a better solubility of intermediate sol (and/or gel) particles before cross-linking appears (Figure 1b). A slower polymerization is in accordance with the higher concentration of the slower polymerizing acrylic acid monomer.[88] The surface of the transparent OG5-15 with the highest amount of acrylic acid appears as a dense, nonporous film. Only smaller NiPAAm-rich domains will have formed, which will not precipitate below the LCST during synthesis but lead to the opaque hue after temperature increase (vide supra; Figure 1c).

Influence of Gel Composition on the Swelling Behavior

As stated, the objective of this study is to develop a chemoresponsive gel for use in a smart valve, here initially for a reaction system comprising an esterification of linear alcohols with linear acids. The gel should therefore show a variation of swelling in esters relative to alcohols and acids and in their mixtures. The choice of NiPAAm and AA monomers, both with a hydrogen-bonding motif, seemed a logical first choice for the purpose.

The swelling of the OG gels was mapped in a series of linear alcohols, carboxylic acids, and the corresponding esters. All gels showed a reversible swelling−shrinkage behavior upon change of the medium from esters to alcohol/acid and back (Figure 2). Structural changes (coil to globule state transitions)[132−134] were not assessed, and the effects are described phenomenologically in this first study.

The degree of swelling (DoS) reaches up to a range of 20 and more, illustrating that some of the organogels are diluted to a level of 5 wt % of polymer segments. The DoS generally is higher in a medium of molecules with a higher concentration of polar entities (i.e., compounds with a lower carbon number; Figure 2).[65] The interactions of larger enthalpy inside the gel are between polar entities, which are more readily replaced by comparable interactions with the solvent medium.[122] The maximum DoS in those solvents tends to higher values for gels with a higher acrylic acid content. The swelling in esters is smaller than that in alcohols, and the difference is more pronounced with higher AA content. These coarse effects are modulated by the specific properties of individual solvents.

A more specific insight is obtained by considering the equilibrium swelling in difference to the situation in the respective C# esters (nos. 1−4; the number in esters refers to the carbon atoms of the carbon chains). The difference from the DoS in esters is higher in gels with a larger acrylic acid content (Figure 3: larger bars). The OG15-5 beads swell to a higher degree in alcohols than in esters and, in contrast, more in esters than in acids (of the same carbon count). The OG10-10 beads show a shift toward larger swelling in alcohols, and the swelling in acid and ester approach each other. This trend is followed in the OG5-15 gel, which swells to comparable degrees in both alcohols and acids. The higher the content of AA, the stronger the interactions with acids.

The solvation of chain segments/globular structures of the copolymer in 1:1 mixtures (by volume) of acids and alcohols has an opposing trend to the swelling in acids, i.e., the relative DoS in NiPAAm-rich gels is higher on average. The swelling of OG15-5 gels in the mixture is even higher than in neat alcohols, in particular for those with a higher carbon count (those with the most hydrophobic interactions). The swelling of OG10-10 in the alcohol−acid mixture is close to that in the derived ester and that of OG5-15 is clearly below that of the individual compounds. The latter is a case of cononsolvency. It remains to be investigated, where the cononsolvency finds its origin, it was argued that any segment in a copolymer may undergo a solvent-driven transition, although an interaction between PNiPAAm and ethanol seems of high impact (surpassing the interactions between acid entities, vide infra).[83]

The observed shrinkage of the organogel in ester-rich environments, relative to alcohols and only partly to acids or mixtures of acids and alcohols, coarsely aligns with its intended function as a smart valve in esterification reactions. The composition during the progress of an esterification reaction would dynamically modulate the swelling state. The behavior of the gels, however, appears not simple to predict along the composition of an esterification reaction mixture. A decent response can be expected for the C2-based reagents, and the study was progressed in that sense with the common reagents of ethanol, ethyl acetate, and acetic acid. These are also less toxic and more stable than the C1 counterparts. This choice was also based on the future option of establishing equilibrium between the C2 reactants and the transesterification product under the action of enzymes.

https://doi.org/10.1021/acs.macromol.6c00960
Macromolecules 2026, 59, 8403−8419

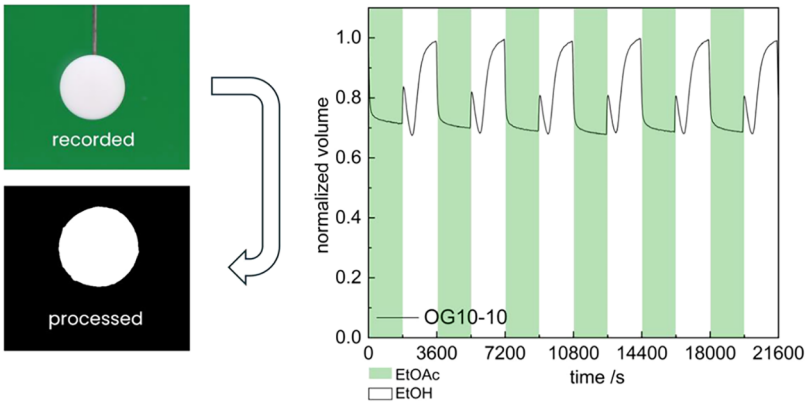

Figure 4. Photographic and Python-script processed image (left) for calculating the average diameter. Normalized volume of OG10-10 over 6 cycles, changing between ethanol and ethyl acetate (right).

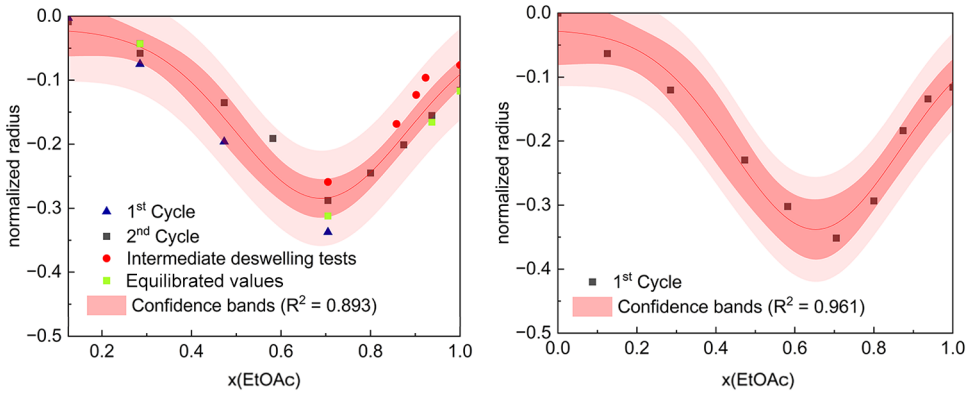

Figure 5. Left: Radius of OG10-10 in EtOH/EtOAc mixtures at 25 °C, normalized to the radius in ethanol; *x*: molar fraction (averaged extrapolated end values from the first cycle, respectively, from 5 consecutive swelling−shrinkage cycles and averaged data of 3 swelling−shrinkage cycles, and equilibrated values). Right: normalized radius of OG10-10 in 1:1 volumetric binary mixtures of acetic acid−ethanol with EtOAc and equilibrated values.

Extent and Kinetics of Swelling−Shrinkage

Method of Detection. The dynamics of the response of the gels to solvent exchange between ethanol and ethyl acetate at 25 °C was addressed to begin with a useful smart valve to show a response in a time frame of minutes.[34] The dynamics of swelling/shrinkage were assessed using a camera-based routine of single-bead-size determination.[51] Images were taken initiated by a computer controller at preset intervals. These were analyzed for the number of pixels of the bead using a python script from which the diameter was calculated. The beads were hanging from a thin metal skewer in a solvent-filled cuvette inside a photo box at room temperature. Measurements could thus routinely be carried out, usually with a 30 min of exposure to a specific solvent or solvent mixture.

For example, a gel bead of OG10-10 expanded in ethanol shrinks when placed in ethyl acetate (Figure 4). The reaction is most dynamic within the first 3 minutes after which the process becomes slower. This is quite general for gels and can be described by multiple exponential or polynomial functions.[48,50,51,135] A consecutive placement in ethanol (changing the cuvette) results in a volume increase. In this special case, the initial reswelling in ethanol is interrupted intermediately by a shrinkage that soon follows by the main swelling phase.[40] The process of switching solvents (periods of 30 min of exposure) can be repeated several times. The response of the gels over 6 cycles is almost identical, illustrating the robustness of the beads and their response.

Cononsolvency Behavior in Ethyl Acetate−Ethanol and Ethyl Acetate−Ethanol−Acetic Acid. The swelling of ethyl acetate-conditioned beads in ethanol is an expected result of the enthalpically driven extension of the gel into ethanol in which it is better soluble. The observed anomaly of an intermediate volume shrinkage must be related to a decrease in the solvent quality for the polymer (segment). This would imply that mixtures of ethanol and ethyl acetate, which form inside the beads, are worse solvents than either component (cononsolvency). The diffusivity of ethanol in ethyl acetate is higher than vice versa (SI), and a gross net flux of ethanol into the bead is expected in any situation with the result that mixtures of the solvents are formed inside the beads. The ethyl ester in the beads also will continue to diffuse into the bulk of ethanol, leading to the final state.

It indeed is found that the beads are smaller (lower DoS) in mixtures of ethyl acetate and ethanol up to a volume ratio of about 4 to 1 (Figure 5): a lower or higher ethyl acetate content leads to beads with a larger equilibrium swelling. The maximum shrinkage in compositions with low amounts of ethanol shows a linear dependence on the molar composition and vice versa for the ethanol-rich regime with a change of trend at a molar fraction of about 0.7 (corresponding to the volume ratio of ethyl acetate/ethanol of 4/1). The data from various measurements show some spread as indicated in Figure

https://doi.org/10.1021/acs.macromol.6c00960
Macromolecules 2026, 59, 8403−8419

5, which is most likely related to the spread in the properties of the beads that are not fully identical in size and structure on account of the drop size and the precipitation polymerization progress.

The shape of the dependence is the typical cononsolvency behavior of PNiPAAm containing beads, known, e.g., in water/methanol or water/ethanol mixtures.[40,76,80−82,132,136,137] This also suggests that parts of the NiPAAm segments of the gel are actively involved in solvation, although it has been put forward that this does not necessarily need to be the case.[83] Such a cononsolvency of NiPAAm-AA copolymers in different organic solvents appears not to have been noticed so far. Apparently, hydrogen bonding to ethanol leads to a situation where the presumably solvated NiPAAm (or AA) domains collapse more extensively (more interactions) in the mixture. A similar behavior is found in ethanol−acetic acid mixtures with a fixed volumetric ratio of 1:1 for swelling and ethyl acetate/ethanol mixtures for shrinkage (Figure 5, right). The smallest size is found at an ethyl acetate fractional molar content a bit lower at 0.65 but close to the 0.7 of ethanol−ethyl acetate situation. Although the absolute radii of the beads are smaller in the ethanol−acetic acid 1:1 mixture (as neat acetic acid has a lower DoS than ethyl acetate), the relative decrease of radius in the minimum of the cononsolvency is comparable (somewhat larger). The interaction with ethanol seems, therefore, of high importance.

No transient swelling−shrinkage of the gels in this study was observed in mixtures of ethyl acetate and ethanol with a volume ratio smaller than 4 to 1. The latter ratio was used to determine the response of the different OG-gel beads to a change to ethanol and ethyl acetate:ethanol as solvating media (Figure 6). A trifold consecutive exchange of solvent

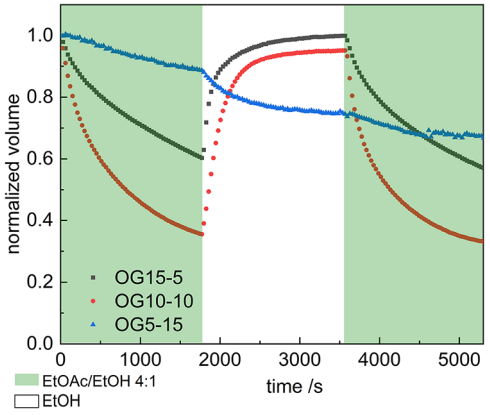

Figure 6. Shrinkage−swelling−shrinkage cycle of the OG-gel beads in ethanol (swelling) and in a mixture of ethyl acetate and ethanol at a vol:vol ratio of 4:1 (shrinkage).

(equilibrated in ethanol, shrinkage in EtOAc/EtOH 4/1−swelling in ethanol−shrinkage) was carried out, each with 30 min of exposure. It is observed that the open-pore gels (Figure 1) respond much faster, and also that OG10-10 has a larger response.[138] The apparent closed surface gel OG5-15 needs about 24 h after shrinkage in the EtOAc/EtOH mixture 4:1 (Figure S5). It shows an erratic behavior in the consecutive 30 min of exposure. These findings highlight the crucial role of monomer composition and morphology from the polymerization process in optimizing the reversibility (and long-term stability) of organogels for solvent-driven applications.[74]

Rates and Magnitude of DoS of the Organogel. The time-dependent volume change of the macroporous organogels can be reasonably well-described by a sum of two exponential decay or growth functions (Table 2). The course of the

Table 2. Time Constants τ_1 and τ_2 at 25 °C of Exponential Description[a]

organogel	shrinkage τ_1 [1000 s]	swelling τ_1 [1000 s]	shrinkage τ_2 [1000 s]	swelling τ_2 [1000 s]
OG15-5	0.17	0.19	2.6	0.7
OG10-10	0.15	0.5	0.9	0.7
OG5-15	2.6		2.6	

[a]From 12 periods of 30 min, radius $a(t)$ fitted to $A_{\tau 1}$ exp $(-t/\tau_1)$ + $A_{\tau 2}$ exp $(-t/\tau_2)$ + A_0

shrinkage of the turbid OG15-5 and OG10-10 gels thus could adequately be fitted by a biexponential decay function (Figure S6). Evaluation of the time curves gives, for the initial fast processes, a factor between swelling and shrinkage rate of 1.1 for OG15-5 to 3 for OG10-10, and a ratio of 4 and 14, respectively, for the slower exponential process. The shrinkage comes with the expulsion of solvent and is slower, the larger the swelling was (as in OG10-10). Note that the maximum shrinkage from ethanol to ethyl acetate−ethanol 4/1 is not reached within the 30 min of observation.

The largest difference between the maximum swelling and most extensive shrinkage with relevant rates is found in the OG10-10 gel. This gel responds reasonably fast to a change in solvent, and the response in 30 min adds up to a 64% change in volume. This gel was therefore selected for a more elaborate investigation as it is potentially useful in a chemical-responsive valve. OG5-15 has a time constant for the swelling process of over 24 h, not really compatible with the objectives of use in a smart valve.

Shrinkage from Ethanol in Ethyl Acetate and in Its Mixtures with Ethanol. The longevity of the OG10-10 gel was indicated in six cycles of shrinkage in 4:1 and 1.5:1 ethyl acetate/ethanol (v/v) mixtures and reswelling in ethanol. It can be observed for the repetitive swelling of OG10-10 in ethanol and shrinkage in an ethyl acetate−ethanol 4:1 mixture that the maximum normalized volume increases to approximately 96% of the original volume in the first cycle and then remains constant over the next five cycles (Figure 7). The shrinkage in 1.5:1 ethyl acetate−ethanol mixture shows some smaller variations in final values, but all-in-all a very consistent response is found too, like in the switching between ethanol and neat ethyl acetate shown in Figure 4. The medium to fast consistent swelling and shrinkage behavior over multiple cycles demonstrates the potential for reliable and repeatable flow control in dynamic chemical environments.

Further characterization of the chemical response behavior of the OG10-10 gel was carried out by the cyclic swelling−shrinkage in ethanol and ethyl acetate−ethanol mixtures of 0.67:1 and 0.25:1 (vol:vol). A similar behavior to that in the 4:1 mixture was observed, with the shrinkage in ethyl acetate−ethanol mixtures becoming smaller at a higher ethanol content (Figure S7).

The time-dependent swelling and shrinkage of the OG10-10 gels by change of the solvent medium between ethanol and ethanol−ethyl acetate mixtures were evaluated by separate fitting of the two phases to exponential functions. A comfortable fitting is reached with a three-parameter approach,

https://doi.org/10.1021/acs.macromol.6c00960
Macromolecules 2026, 59, 8403−8419

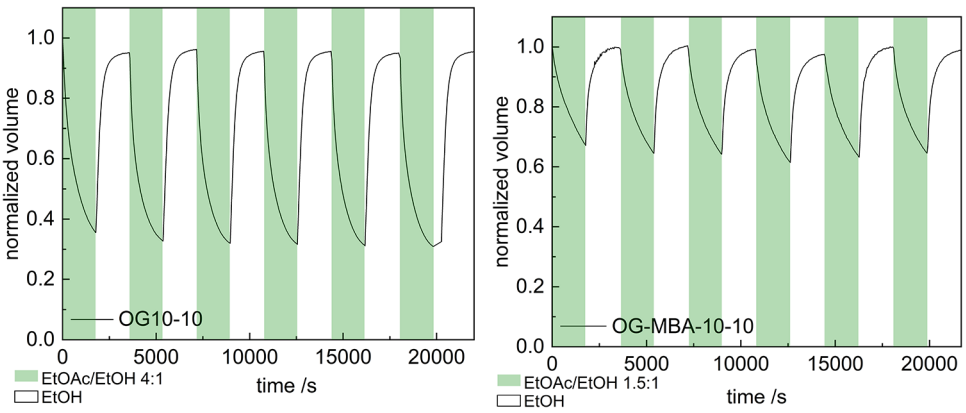

Figure 7. Volume-normalized (to ethanol-swollen bead) dynamic swelling and shrinkage of OG10-10 under cyclic solvent exchange at 25 °C from (a) 4:1, and (b) 1.5:1 EtOAc:EtOH mixture (green underlay) to EtOH (no underlay).

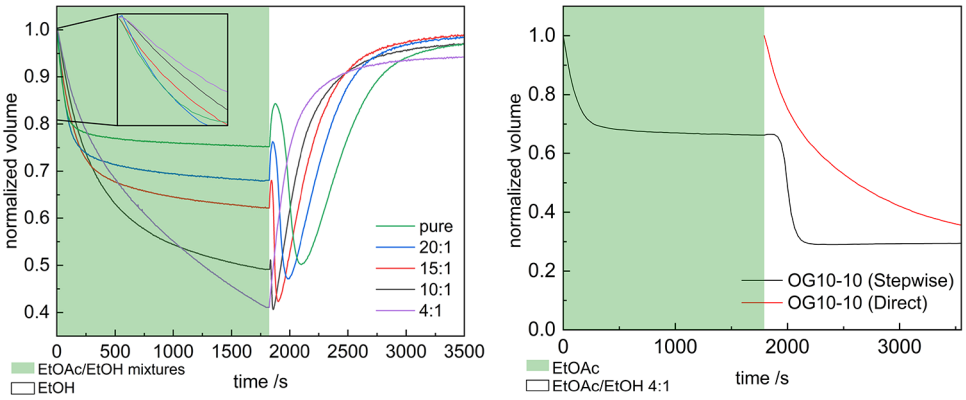

Figure 8. Normalized shrinkage of the volume of OG10-10 beads equilibrated in ethanol in EtOAc/EtOH mixtures, and subsequent swelling in ethanol (left); two-stage shrinkage in ethyl acetate (30 min) and subsequent shrinkage in ethyl acetate/ethanol 4/1 mixture (black) and direct shrinkage in ethyl acetate/ethanol 4/1 mixture (red curve; right).

Table 3. Details of the Shrinkage of Ethanol-Swollen OG10-10 in Ethyl Acetate−Ethanol Mixtures

		first phase				second phase			
vol EtOAc to EtOH	length [s][a]	rel. shrinkage[b] [%]	τ_1 [1000 s]	diffusion time [1000 s][c]	rel. viscosity[d]	τ_2 [1000 s]	Δa_{max} [%][e]	EtOH content[f] [wt %]	excess EtOH[g] [wt %]
neat	135	87	0.1	3.5	1	0.70[h]	9	12	12
20	175	78	0.1	3.7	1.03	0.64	12	13	8
15	285	73	0.16	4.1	1.04	0.56	15	16	9
10	360	63	0.26	4.3	1.06	0.78	23	26	16
4	356	22	0.53	4.9	1.14	2.5	45	36	14
3/2					1.33	2.2	21	n.d	
2/3					1.65	2.4	8	n.d.	
1/4					2.17	n.d.	<1	n.d.	

[a]Time at equal values of the exponential fits of the first and second phases. [b]First phase shrinkage relative to the total shrinkage in the medium after 30 min. [c]Calculated time for diffusion of ethanol over the radius of the bead. [d]Relative viscosity to ethyl acetate, measured at 22 °C. [e]Calculated maximum shrinkage from the simulation. [f]Relative ethanol content within the bead after 30 min of shrinkage, determined using ^{1}H NMR spectroscopy. [g]Excess of ethanol with respect to the bulk medium. [h]Small second phase with about 300 s error. n.d.: not determined or not assessable.

fitting the first and second phase of the time-dependent change of the radius a_t independently to $a_t = A_1 \exp(-t/\tau_{1or2}) + A_2$. The relative (to the initial bead radius) time-dependent swelling (and shrinkage) data of 5 cycles after the initial ones were therefore averaged first. The residuals of the differences between the fit function and data were minimized for values of A_1, A_2, and τ. The approach gives straightforward values for the variables (Table S1). The designation of first respectively the second phase data point were chosen by a criterion that any residual of fit and data points are smaller than an arbitrary 10 times the average residual (clear outliers were also discarded: see Data Availability Statement). The value for $\tau_{1\,or\,2}$ varies within 10% if other cut-offs than the 10% of the residuals are used. The error in the numerical values of τ is thus estimated to be in the range of 10−15%. The beads show some smaller variations in properties too, and the internal structure and size are similar but not the same (Figure 5).

https://doi.org/10.1021/acs.macromol.6c00960
Macromolecules 2026, 59, 8403−8419

The initial rate of shrinkage of the ethanol-swollen beads (after synthesis and conditioning) in ethyl acetate and its mixtures with ethanol is fast, in particular, when the ethanol content in the mixture is low or zero (Figure 8). The shrinkage of ethanol-conditioned OG10-10 gels in ethyl acetate and ethyl acetate with up to 1/4 volumetric part of ethanol can reasonably well be described by the two exponential decays (with rate constants of the first and second phases that approach each other, more ethanol is present; Table 3). The end of the first phase is also the start of the second phase, which is defined here as the moment that the two exponential fit functions of respective initial and final radius simulations have the same magnitude (Figure S8). The shrinkage in mixtures of ethyl acetate with more ethanol has a negligible short initial fast phase and is only described by one exponential for the major part. The time constant then is that of the second phase.

The extent of shrinkage is negatively correlated to the ethanol content of the new medium with ethyl acetate along a natural logarithmic function, i.e., along the chemical potential (Figure 9). This holds true for both the shrinkage in the first fast period and the ultimate shrinkage (calculated). The dependence indicates a proportional amount of ethanol remaining in the gel. This was also confirmed by NMR spectroscopic analysis of the equilibrated and pulverized shrunken beads (Table 3). The beads contain the components of the medium in their channels and pores and inside the swollen walls. It is found that the relative amount of ethanol in the bead always surpasses that of the medium (Table 3, last column), with a trend toward higher numbers for a medium with a higher ethanol concentration. Note that the beads have different swollen sizes, with the consequence that the polymer content is lower at a higher degree of swelling, skewing the comparison somewhat.

The interactions of ethanol with the polymer segments apparently become more abundant with the amount of ethanol in the mixture with predominantly ethyl acetate (up to EtOAc:EtOH of 4:1). A straightforward interpretation is that two types of physical (linking) interactions between the polymer segments exist with different enthalpies: a mutual one between segments and one additionally involving ethanol. This hypothesis shall here not be stressed beyond the point that the gel will change its properties in dependence on the content of ethanol. This kind of description is not uncommon, and similar argumentation is raised for the cononsolvency of PNiPAAm hydrogels in water with ethanol or methanol.[75,76,80,81,83,85]

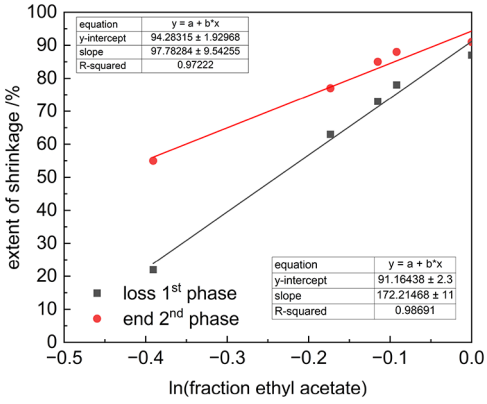

Figure 9. Fraction of ethyl acetate in the medium vs the extent of shrinkage in the first phase and final shrinkage (extrapolated).

The fastest shrinkage of the OG10-10 beads in the first phase is in the transition from the ethanol-swollen state to neat ethyl acetate (Figure 8 inset). This phase of shrinkage lasts for about 2 min to reach 87% of its final value in ethyl acetate. Such a fast response in macroporous PNiPAAm gels is not without example: The response process of a PNiPAAm hydrogel for fast initial shrinkage was reported complete within 100 s for a 3 mm size bead (and for swelling within 400 s) or 200 s for a disk of 4 mm thickness.[74,138,139] (Similar rate data > ∼250 s are found for macroporous polydimethyl acrylamide for a solvent exchange from water to either acetone or dioxane.)[130]

The rate of shrinkage in the first phase is faster with lower ethanol content of the ethyl acetate mixture. The time constant τ_1 and extent (with respect to the final state in the specific mixture) of shrinkage appear negative-linearly correlated (Figure 10). The faster process thus leads to a more extensive shrinkage in the first phase that correlates to the final ethanol content in the bead.

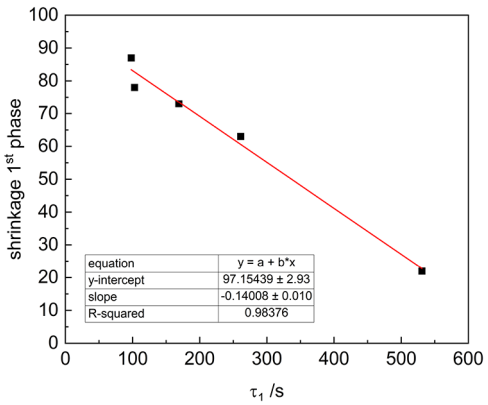

Figure 10. Linear correlation between the extent of relative shrinkage and its time constant of the first phase.

The volumetric change of gel beads will only take place after diffusion of the new medium into the bead.[140] Macroporous gels will react as a result of two processes, the exchange in the pores/channels and subsequently in the structural polymer part. The bead radius of about 3.5 mm and calculated diffusivities of ethanol (SI) for Brownian motion into ethyl acetate−ethanol mixture indicate times of 3−5 × 10^3 s for completion (Table 3; assuming that the effective diffusivity within channels in the range of 5 μm in the structure equals that of the free solvent).[74] The observed rate of loss of the radius in the first phase though is much faster. Other transport mechanisms (convection, surface tension-related effects) than diffusion must contribute to the faster exchange of solvent into the free space of the beads. Calculation of the diffusion of the solvent molecules in the gel walls of approximately 1 μm give a timespan of about 1 s (taking a diffusivity of 10^{-8} cm^2 s^{-1} for movements of the solvent inside the gel walls).[141] This indicates that the exchange of solvent in the channels/pores is rate-limiting, possibly in combination with a small resistance to a flux through the surface of the walls of polymer. This assumption is also corroborated from calculation of the cooperative diffusivity from the theory of swelling $D_{coop} = a_\infty^2/\pi^2\tau_1$ (α_∞ = 1 μm as the equilibrium state of swelling; τ_1 =

https://doi.org/10.1021/acs.macromol.6c00960
Macromolecules 2026, 59, 8403−8419

100 s) gives values of 10^{-11} cm^2 s^{-1} for low concentrations of ethanol, i.e., outside the range of polymer segment−solvent cooperative diffusivities.[50,141] It is in accordance with the finding that the time constants τ_1 have the same order as the viscosity and the diffusion times in about linear correlations (Table 3 and Figure S9). A similar conclusion was drawn for solvent exchange in P(NiPAAm) hydrogels.[130]

The first phase of shrinkage leading to polymer−polymer interactions without (or minor amounts of) ethanol may tentatively be associated with the amount of ethanol that is diluted into the ethyl acetate (rich) medium. The less ethanol that remains in the polymer, the faster the shrinkage and the less compacted the bead becomes. It is compatible with a hypothesis that ethanol diffuses into bulk ethyl acetate (fast effect) and is diluted with ethyl acetate in the channels of the beads. Ethanol is subsequently lost from the polymer segments, which then either become associated with some ethyl acetate or with itself. The extent of ethanol that is initially stripped from the polymer segments is relevant to both the rate and the extent of network collapse. It is inferred that the interactions with remaining ethanol lead to a more compact structure, as described before for PNiPAAm hydrogels with methanol.[83]

A further experiment with OG10-10 showcases how the presence of ethanol influences the swelling/shrinkage of the bead (Figure 11). An ethanol-swollen bead of OG10-10 was

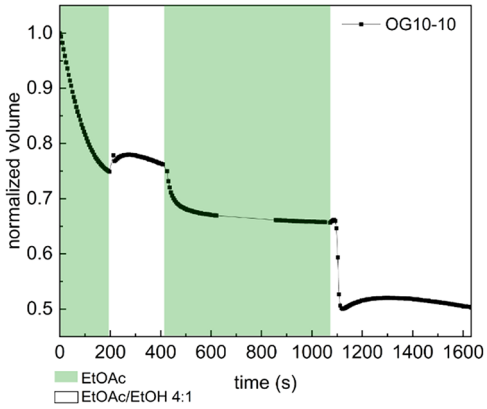

Figure 11. Shrinkage of OG10-10 in ethyl acetate by intermediate suspension in a 4:1 mixture of ethyl acetate:ethanol (by volume).

first shrunk in neat ethyl acetate for 200 s, the time about to reach the end of the first phase of rapid shrinkage. It was subsequently put in a mixture of ethyl acetate:ethanol of 4:1 (by volume). The bead reacts by swelling, i.e., taking up ethanol, instead of pursuing the shrinkage. This shows that an extensive amount of ethanol was previously depleted from the gel. The swelling is shortly (one data point) interrupted by a shrinkage (probably by association of ethanol to polymer segments) and then continues to the initial level (of directly after immersing), before the expected slow shrinkage in that medium sets in. Placing the bead into neat ethyl acetate after another 200 s again results in a fast shrinkage, now to a volume below the level of straightforward shrinkage in ethyl acetate. This shows that the polymer is more compact in the presence of more ethanol. Further exposure of the bead to the ethyl acetate:ethanol 4:1 mixture after the shrinkage in ethyl acetate had basically subsided, again leading to a small swelling by uptake of ethanol and is followed by another fast shrinkage. This is finally followed by a further small ethanol uptake and slow shrinkage. The experiment shows the peculiarities of the organogel in combination with ethanol, which can be understood by assuming two types of polymer−polymer interactions, one with fast dynamics and another involving ethanol with a higher enthalpy and slower character. The slower dynamics of ethanol associated with PNiPAAm is also documented.[122]

The time constants τ_2 of the second phase are in the range of 600−700 s for shrinkage in ethyl acetate:ethanol mixtures down to a ratio of 10:1 (by volume). The time constant becomes larger with more ethanol in the mixture to a value in the range of 2000−2500 s. These values are closer to time expected on the basis of free diffusion of solvents. It may thus be that in this phase of the shrinkage, the diffusion properties of various solvent mixtures take more influence, the diffusivity of ethanol becoming smaller when less ethyl acetate is present (Table 3; SI).

Reswelling in Ethanol. Reswelling in ethanol proceeds almost along an increasing exponential function, with small deviations in the early stages, except for the large expansions from 10:1 and 4:1 ethyl acetate:ethanol volumetric mixtures. The early fast expansion may perhaps be related to ethanol diffusing into the ethyl acetate of the shrunken gel, the reaction of the gel lagging by about 2 min in time. The diffusivity of ethanol in ethyl acetate is larger than vice versa, which would lead to a solvent increase in the bead. The time constants of the second phase or the respective phase in case of one exponential growth function are similar in magnitude. The numbers tend to increase toward a high ethanol content, but otherwise are not too different from each other in the range of ∼300 s (basically within experimental accuracy). The corresponding swelling curves closely match each other, i.e., can almost be superimposed by horizontal shift in that range of smaller changes after the expansion and intermediate shrinkage (Figures 8 and S10). A calculation of the D_{coop} with a_∞ of 3 mm, as the radius of an equivalent nonporous bead, gives a value of about 3.10^{-5} cm^2 s^{-1}. This number is typical for the free diffusion of solvent. The swelling of the macroporous bead thus seems determined by the rate of solvent exchange in the channels/pores, and all other processes are faster.

Intermediate Swelling and Shrinkage. The swelling from beads conditioned in mixtures with more than 90% volumetric parts of ethyl acetate is interrupted by an intermediate shrinkage (Figures 4 and 8). Congruent to the shrinkage, a dependency on the presence of ethanol in the bead exists. Beads with a lower amount of ethanol in the shrunken state swell slower, and over a longer timespan reach a higher level. Ethanol diffuses into the ethyl acetate(:ethanol) swollen beads, to expand the bead to a maximum extent of 4% of the respective radii after shrinkage (the first phase of intermediate reswelling is short and the calculation of rates is not reliable as it comes along with larger errors than the values for time constants). The osmotic pressure is the largest for the beads with the lowest amount of ethanol in ethyl acetate. Thereafter, the bead polymer segments start to react to the ongoing increase of ethanol in the solvent mixture surrounding them. The intermediate quality of the developing solvent mixture in the gel (polymer segments) is lower than after the shrinkage (in the specific mixtures). This makes the beads to lose volume to a minimum before swelling in the medium, with time, more and more ethanol added to the final value. The extent of the intermediate shrinkage (maximum of ∼15% of the radius at the intermediate swelling) again is larger, the

https://doi.org/10.1021/acs.macromol.6c00960
Macromolecules 2026, 59, 8403−8419

lower the ethanol content (and the larger shrunken size) of the bead. Beads with an initially lower ethanol content have a higher driving force for shrinkage in the presence of some additional ethanol (Figure 8, right). The process of intermediate shrinkage is generally slower in the gels shrunk in a medium with less ethanol. Accordingly, the process of shrinkage sustains longer for the gel shrunken in neat ethyl acetate, also with the result that the intermediate shrinkage tends to be more extensive. The timespan scale itself is in the range of 100 s, apparently the time necessary for increasing the ethanol content in the bead and the gel reacting to the change. The lower the amount of ethanol in the gel, the longer the increase of ethanol concentration takes to a level necessary for fast expansion (Table 4).

Table 4. Characteristics of Reswelling OG10-10 Beads in Ethanol

ratio EtOAc–ethanol[a]	time to first max [s]	extent of reswelling [%]	time to inflection point [s][b]	shrinkage [%][c]	τ_2 [100 s]
0	48	4	140	16	3.0
20	30	4	61	15	2.6
15	20	3	25	15	2.4
10	6	1	12	7	2.4
4	~2	n.d.	n.d.		2.5
3/2					3.5
2/3					3.7
1/4					5.4

[a]Medium of shrinkage for 30 min. [b]Intermediate shrinkage, where curves are not symmetrical (Figure 4). [c]Relative to the intermediate maximum; n.d., not determinable.

The overall complex behavior of the beads is a useful one for a smart valve for ethanol-to-ethyl acetate esterification. The change of medium of ethanol as one of the starting materials to the product ethyl acetate goes along with the shrinkage. An accordingly designed valve would open upon conversion (see below). The shrinkage of ethanol-conditioned beads in ethyl acetate–ethanol mixtures proceeds at a higher rate, the more ethyl acetate is formed. The esterification is a rather slow reaction at room temperature, and the response time of the beads would be competitive. Also, the closing of a valve based on the gel in ethyl acetate with fresh ethanol occurs at a satisfactory rate. An increase of the fraction of ethanol in the mixture with ethyl acetate will undergo only a small intermediate shrinkage, if at all. Two further tests were conducted, addressing the impact of the presence of acetic acid and the mechanical stability of the dilute polymer network in a prototype valve.

Behavior of OG10-10 in Ethanol–Ethyl Acetate–Acetic Acid Ternary Mixtures. The ternary system was addressed in a few experiments based on the swelling and shrinkage between ethanol–acetic acid mixtures as a good solvating medium and ethyl acetate for shrinkage. Three compositions were considered with up to a 1:1 volumetric (and about molar) ratio of acetic acid (ethanol else was the major compound; Table 5). The data were similarly treated as for ethanol–ethyl acetate mixtures (Table S2), i.e., fitting to two exponential decay or growth functions. Interesting dependencies appear that need more time to address and are not further discussed in this manuscript.

Table 5. Details of the Shrinkage of OG10-10 from Ethanol–Acetic Acid Mixtures in Ethyl Acetate and the Reverse Swelling

		shrinkage			
vol. ratio[a]	mol fraction EtOH	τ_1 [s]	shrinkage first phase %	τ_2 [1000 s]	total shrinkage[b] %
1:1	0.49	72	85	0.63	31
1:2	0.66	75	88	0.55	35
1:4	0.8	91	87	0.64	31
0:1	1	98	87	0.73	9
		reswelling			
vol. ratio[a]	intermediate swelling[c] %	intermediate shrinkage[d] [100 s]	rate[e] [μm s^{-1}]	intermediate shrinkage[f] [%]	τ_2 [1000 s]
1:1	15	4.7	0.25	11	0.49
1:2	15	4.2	0.31	12	0.45
1:4	17	4	0.39	14	0.39
0:1	4	2.2	1.02	16	0.3

[a]Volumetric ratio of acetic acid to ethanol. [b]Calculated final shrinkage in neat ethyl acetate from exponential fits (±2%). [c]Maximum of the intermediate swelling relative to shrunken starting point (±3% for values >10%). [d]Duration of the intermediate shrinkage. [e]Rate of decrease of the diameter during linear intermediate shrinkage. [f]Extent of intermediate shrinkage relative to intermediate maximum.

Shrinkage in ethyl acetate gave similar observations as of ethanol-swollen beads in ethyl acetate (Figure S11). The presence of acetic acid does not change the role of ethanol in solving the copolymer. A short first phase (<200 s) leads to a close to 90% of the final decrease of the radius. The time constant τ_1 tends to decrease somewhat with the acetic acid content (98 → 75 s). The much slower second phase appears independent from the acetic acid content. The relative final shrinkage itself is more pronounced (30 vs 9%) in the presence of acetic acid, but is not dependent on the concentration in the studied range. The reswelling in the respective mixture of acetic acid and ethanol proceeds with the intermediate shrinkage after a fast swelling (reaching a 15% increase in radius in 2–3 min). The rate of intermediate shrinkage increases with the ethanol concentration, and the extent of shrinkage is linearly correlated to the ethanol concentration and natural logarithm of its fraction (vide supra; Figure S12a). The latter is in accordance with the assumption that ethanol is a factor in the shrinkage. The time constant τ_2 of final swelling is also increasing with the acetic acid concentration, but is in a similar range of 300–500 s (Figure S12b). This lower rate of the second phase itself is satisfactory for the purpose of a smart valve.

Testing the Action of a Smart Valve Based on the OG10-10 Gel

A prototype valve was prepared by putting OG10-10 beads in a glass tubing with a frit at the bottom to stack the beads and also at the top to confine them (Figure 12, left). The medium should be allowed to contact the beads from all directions, as was reasoned before.[40] The close-packed configuration is expected to come along with some leakage, ensuring the prompt exchange of chemical information between the beads and the medium.

The beads were prior-conditioned (shrunken) in ethyl acetate, ensuring that an expansion of the soft material would lead to a loss of free volume between the beads. The prototype valve was vertically connected to a solvent reservoir, which was

https://doi.org/10.1021/acs.macromol.6c00960
Macromolecules 2026, 59, 8403–8419

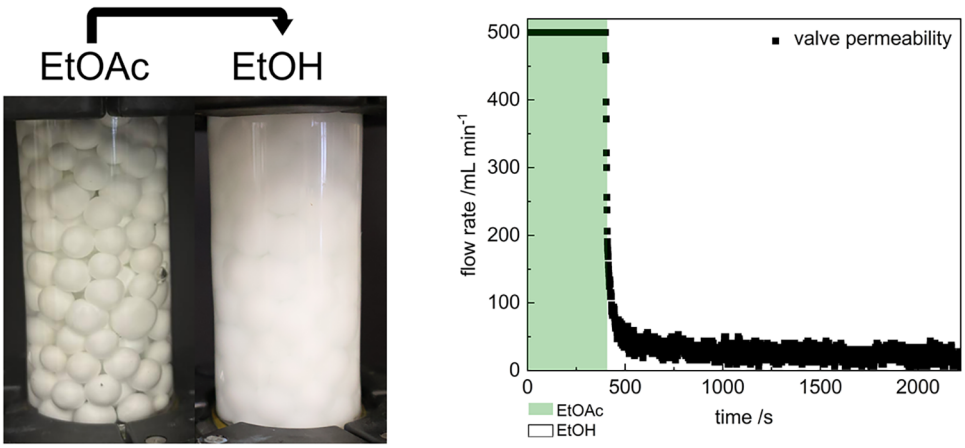

Figure 12. Shrunken and swollen states of the organogel inside the glass casing (left) and the fluid flow rate of the macroscopic valve versus time (right).

initially filled with ethyl acetate. The ethyl acetate was allowed to leave the reservoir at the bottom through the valve in free flow. The level of the solvent in the reservoir was held constant by a pump. The pump volume was metered; it equals the amount of solvent that flowed through the valve.

Ethyl acetate passed the shrunken beads in the casing continuously without much resistance at a rate of about 500 mL min^{-1} (Figure 12). The exchange of solvent in the reservoir to ethanol led to a rapid volumetric expansion of the polymer network, as intended. The expanding spheres filled the available volume inside the casing. A tight physical barrier arises that basically stopped the liquid stream, the pump accordingly running idle, indicating a fully closed state of the valve. The polymer beads, however, appeared mechanically less suitable for further operation. The swelling of the soft polymer beads of mm size pushed them into the rigid stainless steel mesh. Changing the solvent back to ethyl acetate eventually led to the expected shrinkage; however, the compressed polymer structure hindered the rapid solvent exchange throughout the casing. The deformed gels required a longer time for the subsequent shrinkage process. Such material behavior will limit the long-term reversibility in the valve application. Nevertheless, a proof of principle was reached for a smart valve based on the PNiPAAM-AA copolymers. The PNiPAAm-AA copolymers react with a sufficient mechanical answer to a change of medium, i.e., by a change of solvent quality, to operate a macroscopic (primitive) valve. A further development is in progress.

CONCLUSIONS

An effective, simple way to prepare cross-linked gel beads of NiPAAm is elaborated. The beads have a different state of swelling in organic acids, alcohols, and esters, and cononsolvency is a prominent feature when ethanol is involved. The rate of change of the state of swelling makes them potential candidates as smart materials in valves. The UV-droplet polymerization procedure ensures precise bead formation and high reproducibility, making the process scalable for practical applications. The fast polymerization of NiPAAm is essential for the preparation of open-pore beads via the procedure. The ability of macroporous P(NiPAAm-*co*-AA) organogels to reversibly swell and shrink, in particular, in ethanol/acetic acid and ethyl acetate over multiple cycles fulfills some of the prerequisites for a smart valve in an esterification reaction. Overall, the response rate is fast enough for applications in reactions with half-life times of hours (such as an esterification) as a valve, and the unusual transient deswelling would not hamper the functionality. However, the mechanics of the OG10-10 bead are not yet satisfactory for use in the prototype valve. Further research will focus on optimizing monomer compositions to enhance response rates and also the mechanical stability for integrating these materials into microfluidic and macroscopic flow systems for real-time adaptive control: a balance between cross-linking density, response time, and magnitude of response needs to be found.

ASSOCIATED CONTENT

Data Availability Statement

The raw data of the experiments is free of charge at: https://doi.org/10.15480/882.17354.

Supporting Information

The Supporting Information is available free of charge at https://pubs.acs.org/doi/10.1021/acs.macromol.6c00960.

Details in the form of Figures S1−S12 and calculation of the diffusion; the data sets provide a comprehensive overview of the chemical composition, swelling behavior, and kinetic stability of P(NiPAAm-*co*-AA) organogel beads; it serves as the foundational data for analyzing how these gels interact with various organic solvent systems, specifically mixtures of ethyl acetate (EtOAc) and ethanol (EtOH) (PDF)

AUTHOR INFORMATION

Corresponding Author

Gerrit A. Luinstra − *Institute of Technical and Macromolecular Chemistry, University of Hamburg, Hamburg 20146, Germany;* orcid.org/0000-0003-4602-8319; Email: luinstra@chemie.uni-hamburg.de

Authors

Johannes Gmeiner − *Institute of Technical and Macromolecular Chemistry, University of Hamburg, Hamburg 20146, Germany*

Jonah Hasse − *Institute of Technical and Macromolecular Chemistry, University of Hamburg, Hamburg 20146, Germany;* orcid.org/0009-0008-9086-8239

https://doi.org/10.1021/acs.macromol.6c00960
Macromolecules 2026, 59, 8403−8419

Kathrin M. Eckert − *Institute of Thermal Separation Processes, Hamburg University of Technology, Hamburg 21073, Germany;* orcid.org/0000-0002-8454-4886

Irina Smirnova − *Institute of Thermal Separation Processes, Hamburg University of Technology, Hamburg 21073, Germany;* orcid.org/0000-0003-4503-4039

Complete contact information is available at: https://pubs.acs.org/10.1021/acs.macromol.6c00960

Funding

This project is funded by the Deutsche Forschungsgemeinschaft (DFG, German Research Foundation)—SFB 1615-503850735.

Notes

The authors declare no competing financial interest.

REFERENCES

(1) Ansari, M. J.; Rajendran, R. R.; Mohanto, S.; Agarwal, U.; Panda, K.; Dhotre, K.; Manne, R.; Deepak, A.; Zafar, A.; Yasir, M.; Pramanik, S. Poly(N-isopropylacrylamide)-Based Hydrogels for Biomedical Applications: A Review of the State-of-the-Art. *Gels* **2022**, *8* 7 454.

(2) Pasparakis, G.; Vamvakaki, M. Multiresponsive polymers: nano-sized assemblies, stimuli-sensitive gels and smart surfaces. *Polym. Chem.* **2011**, *2* (6), 1234.

(3) Sikdar, P.; Uddin, M. M.; Dip, T. M.; Islam, S.; Hoque, M. S.; Dhar, A. K.; Wu, S. Recent advances in the synthesis of smart hydrogels. *Mater. Adv.* **2021**, *2* (14), 4532−4573.

(4) Beebe, D. J.; Moore, J. S.; Bauer, J. M.; Yu, Q.; Liu, R. H.; Devadoss, C.; Jo, B. H. Functional hydrogel structures for autonomous flow control inside microfluidic channels. *Nature* **2000**, *404* (6778), 588−590.

(5) Wang, S.; Jiao, C.; Gerlach, G.; Körner, J. Porosity Engineering of Dried Smart Poly(N-isopropylacrylamide) Hydrogels for Gas Sensing. *Biomacromolecules* **2024**, *25* (5), 2715−2727.

(6) Grau-Carbonell, A.; Hagemans, F.; Bransen, M.; Elbers, N. A.; van Dijk-Moes, R. J. A.; Sadighikia, S.; Welling, T. A. J.; van Blaaderen, A.; van Huis, M. A. In situ single particle characterization of the themoresponsive and co-nonsolvent behavior of PNIPAM microgels and silica@PNIPAM core-shell colloids. *J. Colloid Interface Sci.* **2023**, *635*, 552−561.

(7) Hruby, M.; Štěpánek, P.; Pánek, J.; Papadakis, C. M. Crosstalk between responsivities to various stimuli in multiresponsive polymers: change in polymer chain and external environment polarity as the key factor. *Colloid Polym. Sci.* **2019**, *297* (11−12), 1383−1401.

(8) Lakshmi, K. N. S.; Vasu Naik, V. V.; Lalitha, K.; et al. An overview of smart characteristics of smart polymers. *World J. Pharm. Pharm. Sci.* **2017**, *6*, 650−663.

(9) Sun, X.; Agate, S.; Salem, K. S.; Lucia, L.; Pal, L. Hydrogel-Based Sensor Networks: Compositions, Properties, and Applications-A Review. *ACS Appl. Bio Mater.* **2021**, *4* (1), 140−162.

(10) Kuzina, M. A.; Kartsev, D. D.; Stratonovich, A. V.; Levkin, P. A. Organogels versus Hydrogels: Advantages, Challenges, and Applications. *Adv. Funct. Mater.* **2023**, *33* (27), No. 2301421, DOI: 10.1002/adfm.202301421.

(11) Wu, Z.; Ding, Q.; Wang, H.; Ye, J.; Luo, Y.; Yu, J.; Zhan, R.; Zhang, H.; Tao, K.; Liu, C.; Wu, J. A Humidity-Resistant, Sensitive, and Stretchable Hydrogel-Based Oxygen Sensor for Wireless Health and Environmental Monitoring. *Adv. Funct. Mater.* **2024**, *34* (6), No. 2308280, DOI: 10.1002/adfm.202308280.

(12) Hennink, W. E.; van Nostrum, C. F. Novel crosslinking methods to design hydrogels. *Adv. Drug Delivery Rev.* **2002**, *54* (1), 13−36.

(13) Chung, H. J.; Lee, Y.; Park, T. G. Thermo-sensitive and biodegradable hydrogels based on stereocomplexed Pluronic multi-block copolymers for controlled protein delivery. *J. Controlled Release* **2008**, *127* (1), 22−30.

(14) Crabbe, A.; Thompson, P. Clinical trial of a patient-operated microwave care system for hydrogel contact lenses. *Optom. Visual Sci.* **2001**, *78* (8), 605−609.

(15) Hejazi, R.; Amiji, M. Chitosan-based gastrointestinal delivery systems. *J. Controlled Release* **2003**, *89* (2), 151−165.

(16) El-Sherbiny, I. M.; Yacoub, M. H. Hydrogel scaffolds for tissue engineering: Progress and challenges. *Global Cardiol. Sci. Pract.* **2013**, *2013* (3), 316−342.

(17) Huang, G. Y.; Zhou, L. H.; Zhang, Q. C.; Chen, Y. M.; Sun, W.; Xu, F.; Lu, T. J. Microfluidic hydrogels for tissue engineering. *Biofabrication* **2011**, *3* (1), No. 12001.

(18) Khan, F.; Tanaka, M.; Ahmad, S. R. Fabrication of polymeric biomaterials: a strategy for tissue engineering and medical devices. *J. Mater. Chem. B* **2015**, *3* (42), 8224−8249.

(19) Kopeček, J. Hydrogel biomaterials: a smart future? *Biomaterials* **2007**, *28* (34), 5185−5192.

(20) Vigata, M.; Meinert, C.; Hutmacher, D. W.; Bock, N. Hydrogels as Drug Delivery Systems: A Review of Current Characterization and Evaluation Techniques. *Pharmaceutics* **2020**, *12* (12), 1188.

(21) Parhi, R. Cross-Linked Hydrogel for Pharmaceutical Applications: A Review. *Adv. Pharm. Bull.* **2017**, *7* (4), 515−530.

(22) Nagase, K.; Yamato, M.; Kanazawa, H.; Okano, T. Poly(N-isopropylacrylamide)-based thermoresponsive surfaces provide new types of biomedical applications. *Biomaterials* **2018**, *153*, 27−48.

(23) Montaser, A. S.; Rehan, M.; El-Naggar, M. E. pH-Thermosensitive hydrogel based on polyvinyl alcohol/sodium alginate/N-isopropyl acrylamide composite for treating re-infected wounds. *Int. J. Biol. Macromol.* **2019**, *124*, 1016−1024.

(24) Haq, M. A.; Su, Y.; Wang, D. Mechanical properties of PNIPAM based hydrogels: A review. *Mater. Sci. Eng., C* **2017**, *70* (Pt 1), 842−855.

(25) Din, M. I.; Khalid, R.; Akbar, F.; Ahmad, G.; Najeeb, J.; Nisa Hussain, Z. U. Recent progress of poly (N-isopropylacrylamide) hybrid hydrogels: synthesis, fundamentals and applications − review. *Soft Mater.* **2018**, *16* (3), 228−247.

(26) Karbarz, M.; Mackiewicz, M.; Kaniewska, K.; Marcisz, K.; Stojek, Z. Recent developments in design and functionalization of micro- and nanostructural environmentally-sensitive hydrogels based on N-isopropylacrylamide. *Appl. Mater. Today* **2017**, *9*, 516−532.

(27) Zhou, X.; Weng, L.; Chen, Q.; Zhang, J.; Shen, D.; Li, Z.; Shao, M.; Xu, J. Investigation of pH sensitivity of poly(acrylic acid- co -acrylamide) hydrogel. *Polym. Int.* **2003**, *52* (7), 1153−1157.

(28) Wang, Y.; Liu, Z.; Han, B.; Dong, Z.; Wang, J.; Sun, D.; Huang, Y.; Chen, G. pH Sensitive polypropylene porous membrane prepared by grafting acrylic acid in supercritical carbon dioxide. *Polymer* **2004**, *45* (3), 855−860.

(29) Ranjha, N. M.; Ayub, G.; Naseem, S.; Ansari, M. T. Preparation and characterization of hybrid pH-sensitive hydrogels of chitosan-co-acrylic acid for controlled release of verapamil. *J. Mater. Sci. Mater. Med.* **2010**, *21* (10), 2805−2816.

(30) Liu, Y.; Velada, J. L.; Huglin, M. B. Thermoreversible swelling behaviour of hydrogels based on N-isopropylacrylamide with sodium acrylate and sodium methacrylate. *Polymer* **1999**, *40* (15), 4299−4306.

(31) Begum, R.; Farooqi, Z. H.; Khan, S. R. Poly(N-isopropylacrylamide-acrylic acid) copolymer microgels for various applications: A review. *Int. J. Polym. Mater. Polym. Biomater.* **2016**, *65* (16), 841−852.

(32) Wang, H.; Wu, X.; Liu, C. S.; Zhu, Z.; Ao, Z.; Zhang, G. Dynamics in N-isopropylacrylamide-acrylic acid copolymer aqueous solution from mechanical spectroscopy. *J. Phys. Chem. B* **2012**, *116* (45), 13411−13415.

(33) Lanzalaco, S.; Mingot, J.; Torras, J.; Alemán, C.; Armelin, E. Recent Advances in Poly(N -isopropylacrylamide) Hydrogels and Derivatives as Promising Materials for Biomedical and Engineering Emerging Applications. *Adv. Eng. Mater.* **2023**, *25* (4), No. 2201303, DOI: 10.1002/adem.202201303.

(34) Lei, M.; Salim, A.; Siegel, R.; Ziaie, B. A hydrogel-actuated microvalve for smart flow control. *Conf. Proc. IEEE Eng. Med. Biol. Soc.* **2004**, *2004*, 2041−2044.

(35) Romero, M. R.; Arrua, R. D.; Alvarez Igarzabal, C. I.; Hilder, E. F. Valve based on novel hydrogels: From synthesis to application. *Sens. Actuators, B* **2013**, *188*, 176−184.
(36) Romero, M. R.; Wolfel, A.; Igarzabal, C. I. A. Smart valve: Polymer actuator to moisture soil control. *Sens. Actuators, B* **2016**, *234*, 53−62.
(37) Gargava, A.; Arya, C.; Raghavan, S. R. Smart Hydrogel-Based Valves Inspired by the Stomata in Plants. *ACS Appl. Mater. Interfaces* **2016**, *8* (28), 18430−18438.
(38) Baldi, A.; Gu, Y.; Loftness, P. E.; Siegel, R. A.; Ziaie, B. A hydrogel-actuated environmentally sensitive microvalve for active flow control. *J. Microelectromech. Syst.* **2003**, *12* (5), 613−621.
(39) D'Eramo, L.; Chollet, B.; Leman, M.; Martwong, E.; Li, M.; Geisler, H.; Dupire, J.; Kerdraon, M.; Vergne, C.; Monti, F.; Tran, Y.; Tabeling, P. Microfluidic actuators based on temperature-responsive hydrogels. *Microsyst. Nanoeng.* **2018**, *4* (1), No. 17069, DOI: 10.1038/micronano.2017.69.
(40) Richter, A.; Howitz, S.; Kuckling, D.; Arndt, K.-F. Influence of volume phase transition phenomena on the behavior of hydrogel-based valves. *Sens. Actuators, B* **2004**, *99* (2−3), 451−458.
(41) Eddington, D. T.; Beebe, D. J. Flow control with hydrogels. *Adv. Drug Delivery Rev.* **2004**, *56* (2), 199−210.
(42) Dong, L.; Jiang, H. Autonomous microfluidics with stimuli-responsive hydrogels. *Soft Matter* **2007**, *3* (10), 1223−1230.
(43) Tevlek, A.; Çetin, E. A. Smart hydrogels in Lab-on-a-Chip (LOC) applications. *React. Funct. Polym.* **2024**, *204*, No. 106023.
(44) Wang, J.; Chen, Z.; Mauk, M.; Hong, K.-S.; Li, M.; Yang, S.; Bau, H. H. Self-actuated, thermo-responsive hydrogel valves for lab on a chip. *Biomed. Microdevices* **2005**, *7* (4), 313−322.
(45) Deligkaris, K.; Tadele, T. S.; Olthuis, W.; van den Berg, A. Hydrogel-based devices for biomedical applications. *Sens. Actuators, B* **2010**, *147* (2), 765−774.
(46) Metze, F. K.; Sant, S.; Meng, Z.; Klok, H.-A.; Kaur, K. Swelling-Activated, Soft Mechanochemistry in Polymer Materials. *Langmuir* **2023**, *39* (10), 3546−3557.
(47) Eckert, K. M.; Müller, S.; Luinstra, G. A.; Smirnova, I. Exploring pNIPAM lyogels: Experimental study on swelling equilibria in various organic solvents and mixtures, supported by COSMO-RS analysis. *Fluid Phase Equilib.* **2024**, *586*, No. 114182.
(48) Nothdurft, K.; Müller, D. H.; Mürtz, S. D.; Meyer, A. A.; Guerzoni, L. P. B.; Jans, A.; Kühne, A. J. C.; Laporte, L. de.; Brands, T.; Bardow, A.; Richtering, W. Is the Microgel Collapse a Two-Step Process? Exploiting Cononsolvency to Probe the Collapse Dynamics of Poly-N-isopropylacrylamide (pNIPAM). *J. Phys. Chem. B* **2021**, *125* (5), 1503−1512.
(49) Steinbeck, L.; Wolff, H. J. M.; Middeldorf, M.; Linkhorst, J.; Wessling, M. Porous Anisometric PNIPAM Microgels: Tailored Porous Structure and Thermal Response. *Macromol. Rapid Commun.* **2024**, *45* (11), No. e2300680.
(50) Sakai, T. Ed. *Physics of Polymer Gels*; Wiley-VCH, 2020.
(51) Bertrand, T.; Peixinho, J.; Mukhopadhyay, S.; MacMinn, C. W. Dynamics of Swelling and Drying in a Spherical Gel. *Phys. Rev. Appl.* **2016**, *6* (6), No. 064010, DOI: 10.1103/PhysRevApplied.6.064010.
(52) Fortes, A. F.; Joseph, D. D.; Lundgren, T. S. Nonlinear mechanics of fluidization of beds of spherical particles. *J. Fluid Mech.* **1987**, *177*, 467−483.
(53) Richter, A.; Klatt, S.; Paschew, G.; Klenke, C. Micropumps operated by swelling and shrinking of temperature-sensitive hydrogels. *Lab Chip* **2009**, *9* (4), 613−618.
(54) Hu, X.; Karnetzke, J.; Fassbender, M.; Drücker, S.; Bettermann, S.; Schroeter, B.; Pauer, W.; Moritz, H.-U.; Fiedler, B.; Luinstra, G.; Smirnova, I. Smart reactors − Combining stimuli-responsive hydrogels and 3D printing. *Chem. Eng. J.* **2020**, *387*, No. 123413.
(55) Yu, Q.; Bauer, J. M.; Moore, J. S.; Beebe, D. J. Responsive biomimetic hydrogel valve for microfluidics. *Appl. Phys. Lett.* **2001**, *78* (17), 2589−2591.
(56) Parimita, S.; Kumar, A.; Krishnaswamy, H.; Ghosh, P. 4D printing of pH-responsive bilayer with programmable shape-shifting behaviour. *Eur. Polym. J.* **2025**, *222*, No. 113581.
(57) Niroumandi, S.; Shojaeifard, M.; Baghani, M. On Single and Multiple pH-Sensitive Hydrogel Micro-valves: A 3D Transient Fully Coupled Fluid−Solid Interaction Study. *Transp. Porous Media* **2022**, *142* (1−2), 295−316.
(58) Argentiere, S.; Gigli, G.; Gerges, M. M. I.; Blasi, L. *Smart Microfluidics: The Role of Stimuli-Responsive Polymers in Microfluidic Devices*, Advances in Microfluidics, Ed.; IntechOpen, 2012.
(59) Sugiura, S.; Sumaru, K.; Ohi, K.; Hiroki, K.; Takagi, T.; Kanamori, T. Photoresponsive polymer gel microvalves controlled by local light irradiation. *Sens. Actuators, A* **2007**, *140* (2), 176−184.
(60) Lee, E.; Lee, H.; Yoo, S. I.; Yoon, J. Photothermally triggered fast responding hydrogels incorporating a hydrophobic moiety for light-controlled microvalves. *ACS Appl. Mater. Interfaces* **2014**, *6* (19), 16949−16955. Published Online: Sep. 25, 2014.
(61) Nagai, D.; Suzuki, A.; Kuribayashi, T. Synthesis of hydrogels from polyallylamine with carbon dioxide as gellant: development of reversible CO(2) absorbent. *Macromol. Rapid Commun.* **2011**, *32* (4), 404−410.
(62) Carretti, E.; Dei, L.; Weiss, R. G.; Baglioni, P. A new class of gels for the conservation of painted surfaces. *J. Cult. Heritage* **2008**, *9* (4), 386−393.
(63) Yu, T.; Wakuda, K.; Blair, D. L.; Weiss, R. G. Reversibly Cross-Linking Amino-Polysiloxanes by Simple Triatomic Molecules. Facile Methods for Tuning Thermal, Rheological, and Adhesive Properties. *J. Phys. Chem. C* **2009**, *113* (27), 11546−11553.
(64) Chen, H.; Zhang, D.; Xiao, S.; Wu, J.; Wei, J.; Tang, Y.; Zhao, C.; Zheng, J. Organogels: Mechanistic insights, design strategies, and translational applications. *Prog. Mater. Sci.* **2026**, *158*, No. 101642.
(65) Komarova, G. A.; Kozhunova, E. Y.; Potemkin, I. I. Behavior of PNIPAM Microgels in Different Organic Solvents. *Molecules* **2022**, *27* (23), 8549.
(66) Eckert, K. M.; Bonsen, J.; Hajnal, A.; Gmeiner, J.; Hasse, J.; Adrian, M.; Karsten, J.; Kißling, P. A.; Penn, A.; Fiedler, B.; Luinstra, G. A.; Smirnova, I. Enhancing swelling kinetics of pNIPAM lyogels: The role of crosslinking, copolymerization, and solvent. *Fluid Phase Equilib.* **2025**, *597*, No. 114462.
(67) Iizawa, T.; Ishido, T.; Gotoh, T.; Sakohara, S. Synthesis of Nonporous Poly(N-alkylacrylamide) Gel Beads by Nonaqueous Sedimentation Polymerization. *Polym. J.* **2007**, *39* (1), 18−20.
(68) Gao, Z.; Grulke, E. A.; Ray, A. K. Synthesis of monodisperse polymer microspheres by photopolymerization of microdroplets. *Colloid Polym. Sci.* **2007**, *285* (8), 847−854.
(69) Wang, M.; Zang, Y.; Hong, K.; Zhao, X.; Yu, C.; Liu, D.; An, Z.; Wang, L.; Yue, W.; Nie, G. Preparation of pH-sensitive carboxymethyl cellulose/chitosan/alginate hydrogel beads with reticulated shell structure to deliver Bacillus subtilis natto. *Int. J. Biol. Macromol.* **2021**, *192*, 684−691. Published Online: Oct. 12, 2021.
(70) Kuckling, D.; Schmidt, T.; Filipcsei, G.; Adler, H.-J. P.; Arndt, K.-F. Preparation of filled temperature-sensitive poly(N -isopropylacrylamide) gel beads. *Macromol. Symp.* **2004**, *210* (1), 369−376.
(71) Dai, Y.-N.; Li, P.; Zhang, J.-P.; Wang, A.-Q.; Wei, Q. A novel pH sensitive N-succinyl chitosan/alginate hydrogel bead for nifedipine delivery. *Biopharm. Drug Dispos.* **2008**, *29* (3), 173−184.
(72) Zhang, H.; Ryu, S. Rotating-liquid-based hydrogel bead generator. *HardwareX* **2020**, *8*, No. e00121.
(73) Sánchez-Moreno, P.; Vicente, J. de.; Nardecchia, S.; Marchal, J. A.; Boulaiz, H. Thermo-Sensitive Nanomaterials: Recent Advance in Synthesis and Biomedical Applications. *Nanomaterials* **2018**, *8* (11), No. 935, DOI: 10.3390/nano8110935.
(74) Alsaid, Y.; Wu, S.; Wu, D.; Du, Y.; Shi, L.; Khodambashi, R.; Rico, R.; Hua, M.; Yan, Y.; Zhao, Y.; Aukes, D.; He, X. Tunable Sponge-Like Hierarchically Porous Hydrogels with Simultaneously Enhanced Diffusivity and Mechanical Properties. *Adv. Mater.* **2021**, *33* (20), No. e2008235.
(75) Zhang, P. Phase Separation of Homopolymers in Binary Mixed Solvents: the Co-Solvency Effect. *Macromolecules* **2025**, *58* (5), 2472−2483.
(76) Scherzinger, C.; Schwarz, A.; Bardow, A.; Leonhard, K.; Richtering, W. Cononsolvency of poly-N-isopropyl acrylamide

(PNIPAM): Microgels versus linear chains and macrogels. *Curr. Opin. Colloid Interface Sci.* **2014**, *19* (2), 84−94.
(77) Zhang, P. Phase Separation of Homopolymers in Binary Mixed Solvents−The Co-Nonsolvency Effect. *Macromolecules* **2024**, *57* (9), 4298−4311.
(78) Wang, J.; Wang, N.; Liu, B.; Bai, J.; Gong, P.; Ru, G.; Feng, J. Preferential adsorption of the additive is not a prerequisite for cononsolvency in water-rich mixtures. *Phys. Chem. Chem. Phys.* **2017**, *19* (44), 30097−30106.
(79) Reitenbach, J.; Wang, P.; Huber, L. F.; Wegener, S. A.; Cubitt, R.; Schanzenbach, D.; Laschewsky, A.; Papadakis, C. M.; Müller-Buschbaum, P. Salt-Mediated Tuning of the Cononsolvency Response Behavior of PNIPMAM Thin Films. *Macromolecules* **2024**, *57* (22), 10635−10647.
(80) Yong, H.; Sommer, J.-U. Cononsolvency Effect: When the Hydrogen Bonding between a Polymer and a Cosolvent Matters. *Macromolecules* **2022**, *55* (24), 11034−11050.
(81) Pérez-Ramírez, H. A.; Haro-Pérez, C.; Odriozola, G. Effect of Temperature on the Cononsolvency of Poly(N -isopropylacrylamide) (PNIPAM) in Aqueous 1-Propanol. *ACS Appl. Polym. Mater.* **2019**, *1* (11), 2961−2972.
(82) Oh, S. Y.; Bae, Y. C. Molecular thermodynamic analysis for reentrant and reentrant-convex type swelling behaviors of thermosensitive hydrogels in mixed solvents. *Polymer* **2013**, *54* (9), 2308−2314.
(83) Mukherji, D.; Marques, C. M.; Kremer, K. Polymer collapse in miscible good solvents is a generic phenomenon driven by preferential adsorption. *Nat. Commun.* **2014**, *5*, No. 4882.
(84) Marcato, D.; Giacometti, A.; Maritan, A.; Rosa, A. Theory of polymers in binary solvent solutions: Mean-field free energy and phase behavior. *Phys. Rev. Mater.* **2024**, *8* (12), No. 125601, DOI: 10.1103/PhysRevMaterials.8.125601.
(85) Li, X.; Wang, Z.; Wang, Z.; Yin, Y.; Jiang, R.; Zhang, P.; Li, B. A novel microscopic origin of co-nonsolvency. *Soft Matter* **2025**, *21* (24), 4858−4868.
(86) Kamli, M.; Guettari, M.; Tajouri, T. Structure of polyvinylpyrrolidone in water/ethanol mixture in dilute and semi-dilute regimes: Roles of solvents mixture composition and polymer concentration. *J. Mol. Liq.* **2023**, *382*, No. 122014.
(87) Grinberg, V. Y.; Burova, T. V.; Grinberg, N. V.; Moskalets, A. P.; Dubovik, A. S.; Plashchina, I. G.; Khokhlov, A. R. Energetics and Mechanisms of poly(N-isopropylacrylamide) Phase Transitions in Water−Methanol Solutions. *Macromolecules* **2020**, *53* (24), 10765−10772.
(88) Xue, W.; Champ, S.; Huglin, M. B. Observations on some copolymerisations involving N -isopropylacrylamide. *Polymer* **2000**, *41* (20), 7575−7581.
(89) Bradley, M.; Vincent, B. Interaction of nonionic surfactants with copolymer microgel particles of NIPAM and acrylic acid. *Langmuir* **2005**, *21* (19), 8630−8634.
(90) Singh, N.; Lyon, L. A. Synthesis of Multifunctional Nanogels Using a Protected Macromonomer Approach. *Colloid Polym. Sci.* **2008**, *286* (8−9), 1061−1069.
(91) Snowden, M. J.; Chowdhry, B. Z.; Vincent, B.; Morris, G. E. Colloidal copolymer microgels of N-isopropylacrylamide and acrylic acid: pH, ionic strength and temperature effects. *J. Chem. Soc. Faraday Trans.* **1996**, *92* (24), 5013−5016.
(92) Lue, S. J.; Chen, C.-H.; Shih, C.-M. Tuning of Lower Critical Solution Temperature (LCST) of Poly(N-Isopropylacrylamide-co-Acrylic acid) Hydrogels. *J. Macromol. Sci., Part B:Phys.* **2011**, *50* (3), 563−579.
(93) Siband, E.; Tran, Y.; Hourdet, D. Thermoresponsive Interpolyelectrolyte Complexation: Application to Macromolecular Assemblies. *Macromolecules* **2011**, *44* (20), 8185−8194.
(94) Ramírez-Irigoyen, A. J.; García-Verdugo, K. F.; Castillo-Ortega, M. M.; Rodríguez-Félix, D. E.; Encinas, J. C.; Plascencia-Jatomea, M.; Argüelles-Monal, W.; Sauceda, I. S.; Pérez-González, R.; Del Castillo-Castro, T. Study of thermal transitions of copolymers based on N -isopropylacrylamide and acrylic acid with potential for curcumin-controlled release. *J. Appl. Polym. Sci.* **2023**, *140* (35), No. e54338, DOI: 10.1002/app.54338.
(95) van Herk, A. General Aspects of Copolymerization. In *Synthesis and Applications of Copolymers*; Parthiban, A., Ed.; Wiley, 2014; pp 54−66 DOI: 10.1002/9781118860168.ch3.
(96) Fernandez Bordín, S. P.; Rufeil Fiori, E.; Padró, J. M.; Galván Josa, V. M.; Plivelic, T. S.; Romero, M. R. Localized Thermoresponsive Behavior in P(NIPAm-co-AAc) Copolymers: Structural Insights From Rheology and Small Angle X-Ray Scattering. *J. Polym. Sci.* **2025**, *63* (2), 393−405.
(97) Khan, A. Preparation and characterization of N-isopropylacrylamide/acrylic acid copolymer core-shell microgel particles. *J. Colloid Interface Sci.* **2007**, *313* (2), 697−704.
(98) Zeinali, E.; Haddadi-Asl, V.; Roghani-Mamaqani, H. Nanocrystalline cellulose grafted random copolymers of N-isopropylacrylamide and acrylic acid synthesized by RAFT polymerization: effect of different acrylic acid contents on LCST behavior. *RSC Adv.* **2014**, *4* (59), 31428−31442.
(99) Minoo-Rabeeh, H.; Hassanzadeh, D.; Azarmi, S.; Entezami, A. A. Effect of synthesis method and buffer composition on the LCST of a smart copolymer of N -isopropylacrylamide and acrylic acid. *Polym. Adv. Technol.* **2007**, *18* (12), 986−992.
(100) Zareie, H.; Volga Bulmus, E.; Gunning, A.; Hoffman, A.; Piskin, E.; Morris, V. Investigation of a stimuli-responsive copolymer by atomic force microscopy. *Polymer* **2000**, *41* (18), 6723−6727.
(101) Chen, G.; Hoffman, A. S. Temperature-induced phase transition behaviors of random vs. graft copolymers of N -isopropylacrylamide and acrylic acid. *Macromol. Rapid Commun.* **1995**, *16* (3), 175−182.
(102) Kim, J. C.; Bae, S. K.; Kim, J. D. Temperature-sensitivity of liposomal lipid bilayers mixed with poly(N-isopropylacrylamide-co-acrylic acid). *J. Biochem.* **1997**, *121* (1), 15−19.
(103) Banerjee, I.; Mishra, D.; Das, T.; Maiti, T. K. Wound pH-responsive sustained release of therapeutics from a poly(NIPAAm-co-AAc) hydrogel. *J. Biomater. Sci., Polym. Ed.* **2012**, *23* (1−4), 111−132.
(104) Bulmuş, V.; Patır, S.; Ali Tuncel, S.; Pişkin, E. Conjugates of poly(N-isopropyl acrylamide-co-acrylic acid) with alanine monopeptide, dipeptide, and tripeptide. *J. Appl. Polym. Sci.* **2003**, *88* (8), 2012−2019.
(105) Jones, M. S. Effect of pH on the lower critical solution temperatures of random copolymers of N-isopropylacrylamide and acrylic acid. *Eur. Polym. J.* **1999**, *35* (5), 795−801.
(106) Yin, X.; Hoffman, A. S.; Stayton, P. S. Poly(N-isopropylacrylamide-co-propylacrylic acid) copolymers that respond sharply to temperature and pH. *Biomacromolecules* **2006**, *7* (5), 1381−1385.
(107) Shieh, Y.-T.; Chen, B.-H.; Wang, T.-L.; Kuo, S.-W. Supercritical CO2 affects the copolymerization, LCST behavior, thermal properties, and hydrogen bonding interactions of poly(N-isopropylacrylamide-co-acrylic acid). *J. Supercrit. Fluids.* **2017**, *130*, 373−380.
(108) Kishi, R.; Kihara, H.; Miura, T. Structural observation of heterogeneous poly(N-isopropyl acrylamide-co-acrylic acid) hydrogels in highly hydrated states. *Colloid Polym. Sci.* **2004**, *283* (2), 133−138.
(109) Teresa Garay, M.; Cristina Llamas, M.; Iglesias, E. Study of polymer-polymer complexes and blends of poly(N-isopropylacrylamide) with poly(carboxylic acid): 1. Poly(acrylic acid) and poly(methacrylic acid). *Polymer* **1997**, *38* (20), 5091−5096.
(110) Ks, S.; Rout, S.; Jacob, A. R. Revisiting crosslinking density effects on pNIPAM microgel properties: Size, electrophoretic mobility, and transition temperatures. *J. Chem. Phys.* **2025**, *162* (18), No. 184903, DOI: 10.1063/5.0269885.
(111) Chourdakis, N.; Bokias, G.; Staikos, G. Poly(N-isopropylacrylamide) grafted to a strongly charged backbone: Thermoresponsive behavior in aqueous solution. *J. Appl. Polym. Sci.* **2004**, *92* (6), 3466−3470.
(112) Hirokawa, Y.; Tanaka, T. Volume phase transition in a nonionic gel. *J. Chem. Phys.* **1984**, *81* (12), 6379−6380.

(113) Xiao, X. C. Effect of the initiator on thermosensitive rate of poly(N-isopropylacrylamide) hydrogels. *Express Polym. Lett.* **2007**, *1* (4), 232−235.
(114) Suzuki, T.; Ikkai, F.; Shibayama, M. Structure and Dynamics of N -Isopropylacrylamide/Acrylic Acid Copolymer Gels Prepared by Cross-Linker-Free UV−Induced Polymerization. *Macromolecules* **2007**, *40* (7), 2509−2514.
(115) Chen, J.; Pei, Y.; Yang, L.-M.; Shi, L.-L.; Luo, H.-J. Synthesis and Properties of Poly(N-isopropylacrylamide-co-acrylamide) Hydrogels. *Macromol. Symp.* **2005**, *225* (1), 103−112.
(116) Park, Y.; Hwang, M.; Kim, M.; Park, E.; Noda, I.; Jung, Y. M. Characterization of the phase transition mechanism of P(NiPAAm-co-AAc) copolymer hydrogel using 2D correlation IR spectroscopy. *Spectrochim. Acta, Part A* **2021**, *252*, No. 119525.
(117) Costa, R. O.; Freitas, R. F. Phase behavior of poly(N-isopropylacrylamide) in binary aqueous solutions. *Polymer* **2002**, *43* (22), 5879−5885.
(118) Wang, L.; Liu, F.; Qian, J.; Wu, Z.; Xiao, R. Multi-responsive PNIPAM-PEGDA hydrogel composite. *Soft Matter* **2021**, *17* (46), 10421−10427.
(119) Pagonis, K.; Bokias, G. Temperature- and solvent-sensitive hydrogels based on N-isopropylacrylamide and N,N-dimethylacrylamide. *Polym. Bull.* **2007**, *58* (1), 289−294.
(120) Dalkas, G.; Pagonis, K.; Bokias, G. Control of the lower critical solution temperature—type cononsolvency properties of poly(N-isopropylacrylamide) in water—dioxane mixtures through copolymerisation with acrylamide. *Polymer* **2006**, *47* (1), 243−248.
(121) Das, A.; Babu, A.; Chakraborty, S.; van Guyse, J. F. R.; Hoogenboom, R.; Maji, S. Poly(N-isopropylacrylamide) and Its Copolymers: A Review on Recent Advances in the Areas of Sensing and Biosensing. *Adv. Funct. Mater.* **2024**, *34* (37), No. 2402432, DOI: 10.1002/adfm.202402432.
(122) Säckel, C.; Klitzing, R. von.; Vogel, M. 2H and 17O NMR studies of solvent dynamics related to the cononsolvency of poly(N-isopropyl acrylamide) in ethanol-water mixtures. *Soft Matter* **2025**, *21* (14), 2738−2747.
(123) Centeno, S. P.; Nothdurft, K.; Klymchenko, A. S.; Pich, A.; Richtering, W.; Wöll, D. FLIM nanoscopy resolves the structure and preferential adsorption in the co-nonsolvency of PNIPAM microgels in methanol-water. *J. Colloid Interface Sci.* **2025**, *678* (Pt B), 210−220.
(124) Backes, S.; Krause, P.; Tabaka, W.; Witt, M. U.; Klitzing, R. von. Combined Cononsolvency and Temperature Effects on Adsorbed PNIPAM Microgels. *Langmuir* **2017**, *33* (50), 14269−14277.
(125) Biswas, C. S.; Patel, V. K.; Vishwakarma, N. K.; Mishra, A. K.; Bhimireddi, R.; Rai, R.; Ray, B. Synthesis, characterization, and drug release properties of poly(N-isopropylacrylamide) gels prepared in methanol−water cononsolvent medium. *J. Appl. Polym. Sci.* **2012**, *125* (3), 2000−2009.
(126) Chung, T.; Im Han, K.; Han, J.; Ahn, K.; Kim, Y. S. Fast and Large Shrinking of Thermoresponsive Hydrogels with Phase-Separated Structures. *Gels* **2021**, *7* (1), No. 18, DOI: 10.3390/gels7010018.
(127) Kishi, R.; Miura, T.; Kihara, H.; Asano, T.; Shibata, M.; Yosomiya, R. Fast pH-thermo-responsive copolymer hydrogels with micro-porous structures. *J. Appl. Polym. Sci.* **2003**, *89* (1), 75−84.
(128) Hauck, N.; Beck, T.; Cojoc, G.; Schlüßler, R.; Ahmed, S.; Raguzin, I.; Mayer, M.; Schubert, J.; Müller, P.; Guck, J.; Thiele, J. PNIPAAm microgels with defined network architecture as temperature sensors in optical stretchers. *Mater. Adv.* **2022**, *3* (15), 6179−6190.
(129) Tamagawa, H. Pores and diffusion characteristics of porous gels. *Polymer* **2000**, *41* (19), 7201−7207.
(130) Pastoriza, A.; Pacios, I. E.; Piérola, I. F. Kinetics of solvent responsiveness in poly(N,N -dimethylacrylamide) hydrogels of different morphology. *Polym. Int.* **2005**, *54* (8), 1205−1211.
(131) Da Silva, R.; Ganzarolli de Oliveira, M. Effect of the cross-linking degree on the morphology of poly(NIPAAm-co-AAc) hydrogels. *Polymer* **2007**, *48* (14), 4114−4122.
(132) Maccarrone, S.; Scherzinger, C.; Holderer, O.; Lindner, P.; Sharp, M.; Richtering, W.; Richter, D. Cononsolvency Effects on the Structure and Dynamics of Microgels. *Macromolecules* **2014**, *47* (17), 5982−5988.
(133) Bharadwaj, S.; Nayar, D.; Dalgicdir, C.; van der Vegt, N. F. A. A cosolvent surfactant mechanism affects polymer collapse in miscible good solvents. *Commun. Chem.* **2020**, *3* (1), No. 165.
(134) Abuwatfa, W. H.; Awad, N. S.; Pitt, W. G.; Husseini, G. A. Thermosensitive Polymers and Thermo-Responsive Liposomal Drug Delivery Systems. *Polymers* **2022**, *14* (5), No. 925.
(135) Schott, H. Kinetics of swelling of polymers and their gels. *J. Pharm. Sci.* **1992**, *81* (5), 467−470.
(136) Schild, H. G.; Muthukumar, M.; Tirrell, D. A. Cononsolvency in mixed aqueous solutions of poly(N-isopropylacrylamide). *Macromolecules* **1991**, *24* (4), 948−952.
(137) Chen, J.-H.; Chen, H.-H.; Chang, Y.-X.; Chuang, P.-Y.; Hong, P.-D. Effects of cononsolvency on preferential adsorption phenomenon in poly(N-isopropylacrylamide) ternary solutions. *J. Appl. Polym. Sci.* **2008**, *107* (4), 2732−2742.
(138) Kabra, B. G.; Gehrke, S. H. Synthesis of fast-response, temperature-sensitive poly(N-isopropylacrylamide) gel. *Polym. Commun.* **1991**, *32* (11), 322.
(139) Zhang, X.-Z.; Chu, C.-C. Thermosensitive PNIPAAm cryogel with superfast and stable oscillatory properties. *Chem. Commun.* **2003**, No. 12, 1446−1447.
(140) Gehrke, S. H. Synthesis, equilibrium swelling, kinetics, permeability and applications of environmentally responsive gels. In *Responsive Gels: Vol. Transitions II*; Dušek, K., Ed.; Springer-Verlag, 1993; pp 81−144 DOI: 10.1007/BFb0021130.
(141) Hansen, C. M. Diffusion in polymers. *Polym. Eng. Sci.* **1980**, *20* (4), 252−258.

https://doi.org/10.1021/acs.macromol.6c00960
Macromolecules 2026, 59, 8403−8419